

---

# Implicit Regularization of Normalization Methods

---

Xiaoxia Wu<sup>\*1</sup> Edgar Dobriban<sup>\*2</sup> Tongzheng Ren<sup>\*1</sup> Shanshan Wu<sup>\*1</sup> Zhiyuan Li<sup>3</sup>  
Suriya Gunasekar<sup>4</sup> Rachel Ward<sup>1</sup> Qiang Liu<sup>1</sup>

## Abstract

Normalization methods such as batch normalization are commonly used in overparametrized models like neural networks. Here, we study the weight normalization (WN) method (Salimans and Kingma, 2016) and a variant called reparametrized projected gradient descent (rPGD) for overparametrized least squares regression and some more general loss functions. WN and rPGD reparametrize the weights with a scale  $g$  and a unit vector such that the objective function becomes *non-convex*. We show that this non-convex formulation has beneficial regularization effects compared to gradient descent on the original objective. We show that these methods adaptively regularize the weights and *converge with exponential rate* to the minimum  $\ell_2$  norm solution (or close to it) even for initializations *far from zero*. This is different from the behavior of gradient descent, which only converges to the min norm solution when started at zero, and is more sensitive to initialization. Some of our proof techniques are different from many related works; for instance we find explicit invariants along the gradient flow paths. We verify our results experimentally and suggest that there may be a similar phenomenon for nonlinear problems such as matrix sensing.

## 1. Introduction

Modern machine learning models often have a large number of parameters, allowing fine-grained adaptation to the data. To prevent over-fitting, a variety of explicit and implicit regularization methods are used. For instance, weight decay shrinks the norms of the weights, thus controlling model complexity. Other regularization methods include

the stochasticity of gradient descent (which may help escape local minima), dropout, and normalization methods such as batch, weight, and layer normalization (Ioffe and Szegedy, 2015; Salimans and Kingma, 2016; Ba et al., 2016).

While these methods are practically popular and successful, their theoretical understanding has only recently started to emerge. An important effect of normalization methods is to make learning more robust to hyperparameters, particularly to the choice of learning rate (Wu et al., 2018; Arora et al., 2019). Moreover, they lead to robustness to the shift and scaling of the inputs, preventing “internal covariate shift” (Ioffe and Szegedy, 2015) and smoothing (Santurkar et al., 2018) or modifying (Lian and Liu, 2019) the optimization landscape.

Here we study an instance of normalization methods specifically in overparametrized least squares regression. In this case, there are infinitely many solutions, and so it is critical that the algorithm converges to one with beneficial properties. When started from zero, it is well known that gradient descent (GD) converges to the minimum Euclidean norm solution, which can be viewed as a good regularization effect. This is suggested both by classical works in numerical analysis (see e.g., Tikhonov regularization), learning theory (Rademacher complexity can sometimes be controlled with norms), as well as more recent direct analyses (Bartlett et al., 2019; Hastie et al., 2019; Belkin et al., 2019; Liang and Rakhlin, 2018). However, this is sensitive to initialization. Our main point is that *normalization provably has a similar regularization effect, which is much more robust to initialization*.

We focus on the weight normalization (WN) (Salimans and Kingma, 2016), which optimizes the weight parameter as  $x = gw/\|w\|_2$  over the length  $g \geq 0$  and the unnormalized direction  $w \in \mathbb{R}^d$  separately. Moreover, inspired by weight normalization, we study a related method where we parametrize the weight as  $x = gw$ , with  $g \geq 0$  and a normalized direction  $w$  with  $\|w\|_2 = 1$ , see e.g., (Douglas et al., 2000). Different from WN, this method performs projected GD (PGD) on the unit norm vector  $v$ , while WN does GD on  $v$  such that  $v/\|v\|$  is the unit vector. We call this variant the *reparametrized projected gradient descent*

---

<sup>\*</sup>Equal contribution <sup>1</sup>The University of Texas at Austin  
<sup>2</sup>The University of Pennsylvania <sup>3</sup>Princeton University  
<sup>4</sup>Microsoft Research, Seattle. Correspondence to: Xiaoxia Wu <xwu@math.utexas.edu>.

(rPGD) algorithm. We show that rPGD and WN have the same limit in continuous time where the stepsize tends to zero, while the two are not identical in discrete time. While the two algorithms stem from prior works, the understanding implicit regularization and convergence properties is still emerging.

Under the setting of overparametrized least squares regression, we show that the WN and rPGD algorithms, in continuous time, have beneficial implicit regularization effects. Namely, they converge to solutions close to the minimum  $\ell_2$  solution. Our proof techniques rely on finding invariants of the continuous time flows, and seem to be interesting and different from many proof methods in the area.

In discrete time, we prove that rPGD can recover the minimum  $\ell_2$  solution with suitable two-phase learning rates, for a wide range of initializations. This goes much beyond GD, which recovers the minimum  $\ell_2$  norm solution *only when the initialization started at zero*. A comparison of WN, rPGD and GD is shown in Figure 1. Moreover, our experiments also show that rPGD has desirable initialization-robust regularization effects for the nonlinear problem of matrix sensing with low-rank solutions. It would be interesting to see how WN and rPGD can be used or motivated a new algorithm in the sparsity domain (Lei et al., 2017).

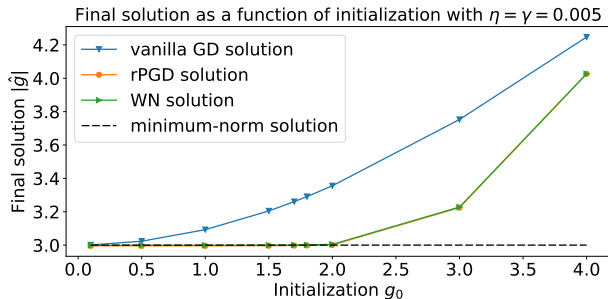


Figure 1: Comparison of the final solutions  $|\hat{g}| = \|\hat{g}\hat{w}\| = \|\hat{x}\|$  provided by GD, WN and rPGD on an overparametrized linear regression problem  $\min_x \frac{1}{2} \|Ax - y\|_2^2$ . All algorithms start from the same initialization  $x_0 = g_0 w_0$ , where  $g_0 \geq 0$  is a scalar, and  $w_0$  is a random unit vector. We run the algorithms until the squared loss is smaller than  $10^{-5}$ . More details about this experiment can be found in Section 5.1. GD converges the minimum  $\ell_2$ -norm solution only when  $g_0 = 0$ , while WN and rPGD converge to the minimum norm solution for a wider range of initializations. The orange, green and black curves overlap when  $0 \leq g_0 \leq 2$ .

While there is a large literature on normalization and implicit regularization (see below), our work differs in crucial ways: first, we are theoretically rigorous, unlike heuristic arguments used in some prior work. Second, we study normalization in the underdetermined case, where there are

many possible solutions (unlike some works focusing on the overdetermined case), and give an exact characterization of the implicit regularization, regardless of the starting point (unlike many papers that study initialization with small norm). Finally, we prove convergence and characterize the solution explicitly (unlike works such as (Gunasekar et al., 2018) that assume convergence to minimizers).

## 1.1. Related Work.

**Implicit regularization.** It has been recognized early that optimization algorithms can have an implicit regularization effect, both in applied mathematics (Strand, 1974), and in deep learning (Morgan and Broulard, 1990; Neyshabur et al., 2014). It has been argued that “algorithmic regularization” can be one of the main differences between the perspectives of statistical data analysis and more traditional computer science (Mahoney, 2012). Furthermore, it has been proposed that “in many large-scale applications it will be more fruitful to understand and exploit what may be termed the statistical properties implicit in algorithms” (Mahoney, 2012). In particular, (Mahoney, 2012) has given examples from graph theory, such as computing the eigenvectors of Laplacians (Mahoney and Orecchia, 2011). This has also been called “algorithmic anti-differentiation” (Gleich and Mahoney, 2014), where the authors presented examples related to finding locally-biased graph partitions.

Theoretical work has shown that gradient descent is a form of regularization for exponential-type losses such as logistic regression, converging to the max-margin SVM for separable data (Soudry et al., 2018; Poggio et al., 2019), as well as for non-separable data (Ji and Telgarsky, 2019). Similar results have been obtained for other optimization methods (Gunasekar et al., 2018), as well as for matrix factorization (Gunasekar et al., 2017; Arora et al., 2019), sparse regression (Vaškevičius et al., 2019), and connecting to ridge regression (Ali et al., 2018). For instance, (Li et al., 2018) showed that GD with small initialization and small step size finds low-rank solutions for matrix sensing. There have also been other arguments that neural networks perform a type of self-regularization, some connecting to random matrix theory (Martin and Mahoney, 2018; Mahoney and Martin, 2019). Other popular methods for regularization include weight decay (a.k.a., ridge regression) (Dobriban and Wager, 2018; Liu and Dobriban, 2019), dropout (Wager et al., 2013), data augmentation (Chen et al., 2019), and others.

**Convergence of normalization methods.** (Salimans and Kingma, 2016) argued that their proposed weight normalization method, optimizing  $w = gv/\|v\|_2$  over  $g \geq 0$  and  $w \in \mathbb{R}^d$ , increases the norm of  $v$ , and leads to robustness to the choice of stepsize. (Hoffer et al., 2018) studied normal-

ization with weight decay and learning-rate adjustments. (Du et al., 2018) proved that GD with weight normalization from randomly initialized weights could recover the right parameters with constant probability in a one-hidden neural network with Gaussian input. (Ward et al., 2019) connected the weight normalization with adaptive gradient methods and proved the sub-linear convergence for both GD and SGD. (Cai et al., 2019) showed that for under-parametrized least squares regression (which is different from our over-parametrized setting), batch normalized GD converges for arbitrary learning rates for the weights, with linear convergence for constant learning rate. Similar results for scale-invariant parameters can be found in (Arora et al., 2018) with more general models, extending to the nonconvex case. (Kohler et al., 2019) proved linear convergence of batch normalization in halfspace learning and neural networks with Gaussian data, using however parameter-dependent learning rates and optimal update of the length  $g$ . (Luo et al., 2019) analyzed BN by using a basic block of neural networks and concluded that BN has implicit regularization. However, none of the above fully explains the implicit regularization in overparametrized linear regression (and in particular our results give precise invariants that are not available in the existing literature).

## 1.2. Our Contributions

Our overall results show that WN and rPGD algorithms in over-parametrized linear regression can converge to a good solution, robust to the scale of initialization, unlike gradient descent. Specifically,

- We give an *adaptive iterative regularization* interpretation of WN and rPGD, which is simple and self-contained.
- We show that for overparametrized least squares, the WN and rPGD algorithms in continuous time have the same limiting flow, called the WN flow (Lemma 3.1). We show that the WN flow converges with exponential rate despite its non-convex nature of the objective function. We precisely characterize the solution of this flow (Theorem 3.2), by finding a nontrivial invariant along its path. This invariant can be generalized beyond linear regression, and only requires that the objective depends only on a low-dimensional subspace (Theorem 3.5).
- Further, we show that with a two-phase schedule, rPGD flow can exactly converge to the min norm solution (Theorem 3.2) for a wide range of initializations. Inspired by rPGD, we study an alternative continuous-time dynamics (the *spherical flow*) that has a similar effect (Theorem 3.3), but is analytically more tractable.

- When the stepsize is not infinitely small, we first consider the simpler setting when the feature matrix is orthogonal and characterize the behavior of rPGD in two phases (Theorem 4.1, Theorem 4.2). We show that by appropriately adjusting the learning rate for the scale  $g$ , the rPGD algorithm converges to the minimum  $\ell_2$  norm solution. Beyond the results obtainable from the continuous time analysis, we give exact iteration complexities for the two phases and provide upper bounds for the stepsize of  $g$ . We extend the result to general data matrices  $A$  (Theorem 4.3), where the results become more challenging to prove and harder to parse (and thus it makes sense to give the results for orthogonal matrices first and separately).
- We support our theory on linear regression with experiments (Section 5.1). We also show experiments supporting convergence to the minimum nuclear norm solution in matrix sensing (Section 5.2), suggesting that the phenomena discovered here may extend to nonlinear problems.

## 2. Setup

Throughout,  $\|\cdot\|$  denotes the  $\ell_2$  norm. The standard over-parametrized linear regression problem can be written as

$$\min_{x \in \mathbb{R}^d} \frac{1}{2} \|Ax - y\|^2, \quad (1)$$

where  $A \in \mathbb{R}^{m \times d}$  ( $m < d$ ) is the feature matrix and  $y \in \mathbb{R}^m$  is the target vector. Without loss of generality, we assume that the feature matrix  $A$  has rank  $m$ . This objective has infinitely many global minimizers, and among them we denote the minimum  $\ell_2$ -norm solution by  $x^*$ . Then  $x^*$  must satisfy the following properties:

- $Ax^* = y$ .
- $x^*$  is in the row space of the matrix  $A$ .

Any global minimizer of (1) that lies in the row space of  $A$  must be the minimum  $\ell_2$ -norm solution. To better illustrate the minimum  $\ell_2$ -norm solution, define  $x = x^{\parallel} + x^{\perp}$  so that

$$Ax^{\parallel} = Ax \text{ and } Ax^{\perp} = 0. \quad (2)$$

Thus the minimum  $\ell_2$ -norm solution satisfies  $x^{*\parallel} = x^*$ .

In this paper, we focus on the normalization methods that reparametrize the convex linear regression to a non-convex problem, using weight normalization and the reparametrized projected gradient descent method, respectively.

**Weight normalization (WN)** Weight normalization (Salimans and Kingma, 2016) reparametrizes the variable  $x$  as  $g \frac{w}{\|w\|}$ , which leads to the following objective function:

$$h(g, w) = \frac{1}{2} \left\| g \frac{Aw}{\|w\|} - y \right\|^2. \quad (3)$$

We can write the minimum-norm solution as  $x^* = g^* \frac{w^*}{\|w^*\|}$ , where  $g^* > 0$  is assumed. Note here that  $w^*$  is not unique, so we simply choose any such  $w^*$ . Also,  $g^* > 0$  can be achieved unless  $x^* = 0$ , which implies that  $y = 0$ ; and we exclude this corner case throughout the paper.

Next, the gradients of the function  $h(g, w) = f(g, w/\|w\|)$  with respect to  $g$  and  $w$  are:

$$\begin{aligned} \nabla_g h(w, g) &= \left\langle \frac{w}{\|w\|}, A^T r \right\rangle \\ \nabla_w h(w, g) &= \frac{g}{\|w\|} \left( I - \frac{ww^T}{\|w\|^2} \right) A^T r \end{aligned}$$

The discrete time WN algorithm is shown in Algorithm 1.

---

**Algorithm 1** WN for the problem in equation 3

---

**Input:** initialization  $w_0$  and  $g_0$ , number of iterations  $T$ , step-sizes  $\gamma_t$  and  $\eta_t$  for  $t = 0, \dots, T - 1$ .

**for**  $t = 0, 1, 2, \dots, T - 1$  **do**  
 $w_{t+1} = w_t - \eta_t \nabla_w h(w_t, g_t)$   
 $g_{t+1} = g_t - \gamma_t \nabla_g h(w_t, g_t)$   
**end for**

---

**Reparametrized Projected Gradient Descent (rPGD)**

Weight normalization updates the vector  $w$ , which can have a norm different from unity. In a sense, this is a bit redundant, because the algorithm only uses  $w/\|w\|$ , i.e., the direction of  $w$ . Inspired by this observation, we investigate the algorithm directly updating the direction of  $w$ . See e.g., (Douglas et al., 2000) for such algorithms; and this can also be viewed as an instance of Riemannian gradient descent. Since the direction is a unit vector, we must perform projected gradient descent on it. Thus, we reparametrize the variable  $x$  as  $gw$ , where  $g \geq 0$  denotes the scale and  $w \in \mathbb{R}^d$  satisfies  $\|w\| = 1$ .

Now we can rewrite equation 1 as minimizing the following loss function

$$f(w, g) := \frac{1}{2} \|Agw - y\|^2, \text{ where } \|w\| = 1. \quad (4)$$

where  $w \in \mathbb{R}^d$  and  $g \in \mathbb{R}$ . We can write the minimum-norm solution as  $x^* = g^* w^*$ , with  $g^* > 0$  and  $\|w^*\| = 1$ . To solve it, we consider projected gradient descent (PGD) (Algorithm 2), and we call this algorithm the reparametrized PGD (rPGD) algorithm in this context.

Algorithm 2 has  $T$  iterations. In each iteration, it first performs a gradient step on the vector  $w$ , followed by a projection (or normalization) step, and then performs a gradient step on the scale  $g$ . Let  $r = Agw - y$  be the appropriate negative residual. The gradients of  $f$  are

$$\nabla_w f(w, g) = gA^T r, \quad \nabla_g f(w, g) = w^T A^T r. \quad (5)$$

---

**Algorithm 2** rPGD for the problem in equation 4

---

**Input:** initialization  $w_0$  and  $g_0$ , number of iterations  $T$ , step-sizes  $\gamma_t$  and  $\eta_t$  for  $t = 0, \dots, T - 1$ .

**for**  $t = 0, 1, 2, \dots, T - 1$  **do**  
 $v_t = w_t - \eta_t \nabla_w f(w_t, g_t)$  (gradient step)  
 $w_{t+1} = \frac{v_t}{\|v_t\|}$  (projection into unit sphere)  
 $g_{t+1} = g_t - \gamma_t \nabla_g f(w_t, g_t)$  (gradient step)  
**end for**

---

**2.1. Normalization Methods as an Adaptive Regularization**

We show that Algorithms 1 and 2 can be viewed as gradient descent on an adaptively  $\ell_2$ -regularized regression problems (a.k.a ridge regression).

**WN.** Let  $x_t = \frac{g_t w_t}{\|w_t\|}$ . Notice that:

$$\begin{aligned} \frac{g_{t+1} w_{t+1}}{\|w_{t+1}\|} &= \frac{g_t}{\|w_t\|} w_t + \left( \frac{g_{t+1}}{\|w_{t+1}\|} - \frac{g_t}{\|w_t\|} \right) w_t \\ &\quad - \eta_t \frac{g_{t+1}}{\|w_{t+1}\|} \frac{g_t}{\|w_t\|} \left( I - \frac{w_t w_t^T}{\|w_t\|^2} \right) A^T r \end{aligned}$$

This can be translated to the update of  $x_t$  as

$$\begin{aligned} x_{t+1} &= x_t - \eta_t \frac{g_{t+1} g_t}{\|w_{t+1}\| \|w_t\|} A^T r \\ &\quad - \left( 1 - \frac{g_{t+1} \|w_t\|}{g_t \|w_{t+1}\|} - \eta_t \frac{g_{t+1}}{\|w_{t+1}\|} \left\langle \frac{w_t}{\|w_t\|^2}, A^T r \right\rangle \right) x_t \end{aligned}$$

**rPGD.** Let  $x_t = g_t w_t$ . The update of  $w_t$  in Algorithm 2 is

$$w_{t+1} = \frac{1}{\|v_t\|} (w_t - \eta_t g_t A^T (Ax_t - Ax^*)). \quad (6)$$

We can now write the update of  $x_{t+1} = g_{t+1} w_{t+1}$  as

$$x_{t+1} = x_t - \frac{\eta_t g_t g_{t+1}}{\|v_t\|} A^T (Ax_t - Ax^*) - \left( 1 - \frac{g_{t+1}}{g_t \|v_t\|} \right) x_t.$$

Both updates can be viewed as a gradient step on the following  $\ell_2$ -regularized regression problem, with specific choices of  $\lambda_t$ :

$$\frac{1}{2} \|Ax - Ax^*\|^2 + \lambda_t \|x\|^2,$$

We see that the regularization parameter changes for each

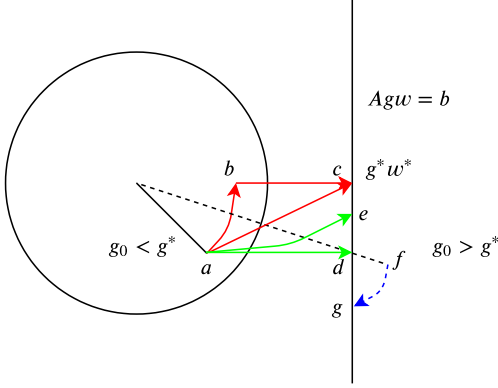


Figure 2: Consider the toy example  $f(w_1, w_2, g) = (gw_1 - 2)^2$ , with minimum-norm solution at  $c = (2, 0)$ . Suppose we start with  $g_0 < g^*$  (point  $a$ ). Then GD converges to  $d$ , while rPGD could result in a point ( $e$  or  $c$ ) closer to minimum-norm  $c$  depending on the stepsize schedule of  $g$ . rPGD and WN could follow one of the red paths  $a \rightarrow b \rightarrow c$  or  $a \rightarrow c$  to the minimum-norm solution. Path  $a \rightarrow b \rightarrow c$  is taken if  $g_0$  is fixed for a certain time, and updated later. The straight line path  $a \rightarrow c$  is taken when we update  $g$  in a careful way. If we do not control  $g$  appropriately, we may end up at  $e$ . If we start with  $g_0 > g^*$ , for instance at  $f$ , we may end up at point  $g$ . See Figure 3 for 3d and contour plots.

iteration for both WN and rPGD, as follows:

$$\begin{aligned} \text{(WN)} \quad \lambda_t &= \frac{\|w_{t+1}\| \|w_t\|}{g_{t+1} g_t} \left(1 - \frac{g_{t+1} \|w_t\|}{g_t \|w_{t+1}\|}\right) \\ &\quad - \eta \frac{g_{t+1}}{\|w_{t+1}\|} \left\langle \frac{w_t}{\|w_t\|^2}, A^T r \right\rangle \\ \text{(rPGD)} \quad \lambda_t &= (g_t \|v_t\| - g_{t+1}) / (\eta_t g_t^2 g_{t+1}) \end{aligned}$$

The regularization parameters are highly dependent on  $g_t$ ,  $g_{t+1}$  and the input matrix  $A$ . However, it is difficult to characterize the behavior of  $\lambda_t$  in general. For the simpler setting of orthogonal  $A$  considered in Section 4, we can see for rPGD that: 1) If the learning rate of  $g$  is small enough, we will have  $g_{t+1} < g_t \|v_t\|$ , which means that  $\lambda_t > 0$ ; 2) When  $g_t w_t$  is close to  $g^* w^*$ , we will have  $\|v_t\| \approx 1$ , and  $g_{t+1} \approx g_t$ , which means that  $\lambda_t \approx 0$ .

### 3. Continuous Time Analysis

In this section, we study the properties of continuous limits of WN and rPGD, to give some insight into the implicit regularization of normalization methods.

#### 3.1. Equivalence of WN and rPGD in continuous limit

We first prove that when taking the continuous limit of the dynamics of  $(g_t, w_t / \|w_t\|)$  for WN, it evolves exactly ac-

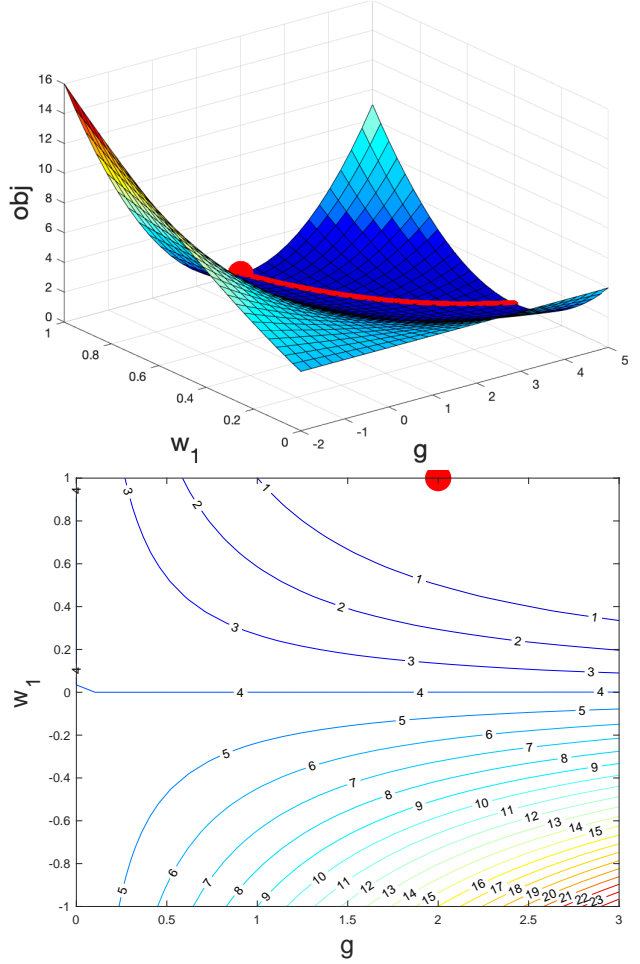


Figure 3: A 3d plot (top) and contour map (bottom) for  $f(w_1, w_2, g) = (gw_1 - 2)^2$ . The red solid dot in both plots is the point  $c = (w_1, g) = (1, 2)$ , the minimum norm solution. The red curve of the top plot represents the solution space where  $gw_1 = 2$ . For any initial value, the algorithms can be tuned to converge to the solution space.

ording to the limit of the dynamics of  $(g_t, w_t)$  for rPGD. So, the two different discrete algorithms have the same continuous limit.

**Lemma 3.1** (Limiting flow for WN and rPGD). *Suppose the stepsizes  $\eta_t, \gamma_t$  are fixed constants  $\eta, \gamma$ . Consider the limit where  $\eta \rightarrow 0$ , and  $\gamma \rightarrow 0$ . Set the initialization  $\|w_0\| = 1$ . For WN (Algorithm 1)  $(g_t, w_t / \|w_t\|)$ , and for rPGD (Algorithm 2)  $(g_t, w_t)$  have the same limiting dynamics, which we called **WN flow**, given by the pair of ordinary differential equations*

$$\dot{g}_t = -\nabla_g f(w_t, g_t), \quad (7)$$

$$\dot{w}_t = -P_{w_t^\perp} \nabla_w f(w_t, g_t). \quad (8)$$

Here  $P_{w^\perp} = I - \frac{ww^\top}{\|w\|^2}$ , is the projection into the orthocom-

plement of  $w$ , while  $\nabla_g f$  and  $\nabla_w f$  are defined in equation 5.

The proof is given in Appendix A.

### 3.2. Convergence and implicit regularization of WN

We next study the convergence and implicit regularization of the WN flow.

**Theorem 3.2** (Convergence of WN flow). *Suppose the smallest eigenvalue of  $AA^T$  is positive.*

- Suppose we initialize the WN flow at  $g_0, w_0$  ( $g_0 > 0$ ), such that  $\|w_0\| = 1$  and

$$2 \log \|w_0^\perp\| + g_0^2 > 0 \quad (9)$$

Then the loss along the WN flow path  $(g_t, w_t)$  decreases geometrically, satisfying

$$f(w_t, g_t) \leq \exp(-t\lambda_{\min}(AA^T)R)f(w_0, g_0)$$

with  $R = \min\{2 \log \|w_0^\perp\| + g_0^2, 1\}$ .

Moreover  $(g_t, w_t)$  converges to the unique point  $g, w$  such that  $gw$  is a global minimizer, and

$$w^\perp = \exp\left(\frac{g_0^2 - g^2}{2}\right) w_0^\perp. \quad (10)$$

- For the constrained dynamics where we keep  $g_0$  fixed and run the WN flow on  $w$  only, subject to the constraint  $\|w\| = 1$ . If  $A$  is orthogonal, i.e.,  $AA^T = I$ , then this converges to the minimum-norm direction, i.e.,  $w_t \rightarrow w^*$ .
- If  $A$  is not orthogonal, then the flow still converges to a point  $\tilde{w}_0$  in the row space of  $A$ . When starting the WN flow from  $g_0, \tilde{w}_0$ , it converges to the minimum-norm solution, i.e.,  $(g_0, \tilde{w}_0) \rightarrow (g^*, w^*)$ .

The proof is in Appendix B. The first part of Theorem 3.2 shows that the WN flow converges to a solution which is not exactly the minimum-norm one. However, if we initialize with  $g_0$  satisfying equation 9, and the solution  $g$  greater than  $g_0$ , then equation 10 implies that the component  $w^\perp$  in the orthocomplement of the row span of  $A$  decreases. In particular  $2 \log \|w^\perp\| + g^2$  is invariant along the path, i.e.,

$$2 \log \|w^\perp\| + g^2 = 2 \log \|w_0^\perp\| + g_0^2.$$

Thus, we get close to the minimum-norm solution. This is in contrast to gradient descent, where  $\|w^\perp\|^2$  is preserved, and we can end up further from the min norm solution. See the end of this section for a concrete example.

The dynamics of  $g_t$  deserve special attention. We emphasize that for large  $g_0$  the flow can get very far from the min

norm solution, see Figure 2. However, the condition in the theorem also requires  $g_0$  not to be small (e.g., equation 9). We think that this may be an artifact of the proof, and that no such condition should be required. In the discrete time analysis from section 4, we will prove that  $g_t > 0$  is increasing for orthogonal matrices  $A$  with  $AA^T = I$ . In general, if  $A$  is well-conditioned, the algorithm guarantees linear convergence close to minimum-norm solution for any  $g_0 \leq \epsilon$ , similar to or better than GD.

The second and third parts of the theorem 3.2 show a distinction between orthogonal and general  $A$ . For orthogonal  $A$ , even fixing the scale  $g_0$  we can converge to the direction of the min norm solution. However, we do not directly recover  $g^*$  in the flow, but this can be recovered afterwards as a postprocessing step by evaluating the norms of the data.

For general  $A$ , if we first keep  $g$  fixed, we do not necessarily converge in the right direction. However, if we run the flow until convergence, and then restart it, then we converge to the min norm solution. This mirrors the results for discrete time presented later. See Figure 2 for an illustration. We mention that the form of the flow for the fixed  $g$  case is well known (e.g. see Section 1.6 in (Helmke and Moore, 2012)), but the convergence results provided there only concern the squared input  $A$ , which is a somewhat limited setting in practice.

### 3.3. A Variant of the WN Flow

Next we study a different and more tractable continuous time version of the rPGD/WN algorithm, given by the dynamics

$$\begin{aligned} \dot{g}_t &= -\nabla_g f(w_t, g_t) \\ \dot{u}_t &= -\nabla_w f(w_t, g_t) \\ w_t &= u_t / \|u_t\|. \end{aligned}$$

This flow is related to, but not exactly the same as, rPGD or weight normalization, that have a different dynamics on  $w_t$ . However, it is simpler to study. We will refer to it as the “**spherical flow**”, because  $w_t$  can be viewed as a flow on the sphere. To be clear, if  $u_t$  ever becomes zero, then we halt the ODE. Discretizing this ODE leads to the usual dynamics for  $g_t$ , and to  $u_{t+1} = u_t - \eta \nabla f_g(w_t, g_t)$ ,  $w_{t+1} = u_{t+1} / \|u_{t+1}\|$ . Thus, this algorithm has an auxiliary variable  $u_t$ . We take a gradient step with respect to  $w_t$  on  $u_t$ , and then update  $w_t$  to be the renormalized result. Thus, this algorithm is somewhat heuristic. However we show that it has good properties. Since  $u_0$  is arbitrary, we choose it to be  $u_0 = w_0 \cdot g_0^2 / 2$  (for reasons explained in the proof).

**Theorem 3.3** (Convergence of spherical flow). *Suppose the smallest eigenvalue of  $AA^T$  is positive. Then the spherical flow path  $(g_t, w_t)$  converges with objective decreasing geometrically at rate  $2\lambda_{\min}(AA^T)$  to a point  $g, w$  that*

solves the system  $Agw = b$ . Moreover, when started from  $g_0, w_0$  ( $g_0 > 0$ ) we find the unique solution of the above system such that

$$g \cdot \|w^\perp\|^2 = g_0 \cdot \|w_0^\perp\|^2.$$

The proof is in Appendix C. We can see that, by constraining the  $w_t$  evolving on the sphere, we can always decrease  $\|w^\perp\|$  if initialized the flow with a small  $g_0$ . Comparing the flows, WN is more robust to initialization than spherical flow. Indeed, WN keeps  $\|w^\perp\|^2 \exp(g^2)$  invariant, and thus when  $g$  increases,  $\|w^\perp\|^2$  decreases much more than for spherical flow.

### 3.4. A Concrete Example

To gain more insight into the regularization effects of the flows, we provide here a simple example, see also Figure 2 for a related example. Suppose we have a two-dimensional parameter  $w$ , and we make a 1-dimensional observation using the matrix  $A = [1, 0]$ , and  $b = 1$ . Suppose moreover that we start with  $w_0 = [0, 1]^T$ . Then, the equation we are solving is  $gw[1] = 1$  (where square brackets index coordinates of vectors), and the minimum norm solution is  $w = [1, 0]^T$ , with  $g^* = 1$ . Suppose now that we start with some other  $g_0$ . Then, it follows that spherical flow converges to the unique  $g, w$  that solves the system such that  $g = g_0/2 + \sqrt{g_0^2/4 + 1}$ . If  $g_0$  is relatively small, this quantity is close to unity (i.e.,  $g^*$ ), so the spherical flow converges close to the true min norm solution. Moreover, WN flow converges to the unique solution  $g, w$  such that  $1/g^2 + \exp(g_0^2 - g^2) = 1$ . This can generally not be solved explicitly; however, it has a stronger regularization effect than spherical flow.

### 3.5. Beyond Linear Regression

Here we illustrate that the invariant in the optimization path holds more generally than for linear regression, and specifically for certain general loss functions that only depend on a small dimensional subspace of the parameter space. Let  $L : \mathbb{R}^d \rightarrow \mathbb{R}$  be the loss function, and our goal is to solve

$$\min_{x \in \mathbb{R}^d} L(x) \quad (11)$$

where  $L(x)$  is differentiable and satisfies following assumption:

**Assumption 3.4** (Low-dimensional gradient). *There exists a projection matrix  $P \in \mathbb{R}^{d \times d}$  such that*

$$(I - P)\nabla L(x) = 0, \forall x \in \mathbb{R}^d;$$

Let  $P^\perp = (I - P)$ . Assumption 3.4 is equivalent to the fact that the gradient of  $L$  lives in the low-dimensional space given by the span of  $P$ ,  $\nabla L(x) \in \text{span}(P)$ . This implies

$$L(x) = L(Px) \quad \forall x \in \mathbb{R}^d.$$

This means that the objective only depends on the projection of  $x$  into the span of  $P$ . To use the orthogonal projection in what follows, define  $x^\parallel = Px$  and  $x^\perp = P^\perp x$ . For the undetermined linear regression,  $P = A^\dagger A$  where  $A^\dagger$  is the pseudo-inverse of the matrix  $A$ .

**Theorem 3.5** (WN flow Invariance for General Loss). *Consider the loss function in equation 11 with Assumption 3.4. The WN method transforms the loss function to  $h(g, w) = L\left(g \frac{w_t}{\|w_t\|}\right)$ . The WN gradient flow from Algorithm 1 with initial condition  $(w_0, g_0)$ , started from  $w_0$  with not necessarily unit norm, has the invariant*

$$w_t^\perp = \exp\left(\frac{g_0^2 - g_t^2}{2\|w_0\|^2}\right) w_0^\perp.$$

The proof of the above theorem is a simple extension of the proof in Part I of Theorem 3.2 with  $A^\top r_t = \nabla L\left(g_t \frac{w_t}{\|w_t\|}\right)$ . This result suggests that the reason for the invariance is that the original objective function before reparametrization only depends on a smaller dimensional space.

## 4. Discrete Time Analysis

In this section, we analyze rPGD for linear regression in discrete time when the step-size is not infinitely small, which is closer to practice. We show that rPGD, with properly chosen learning rates, can converge to a small neighborhood the minimum  $\ell_2$ -norm solution, even when the initialization point is *far away from the origin*. This behavior is quite different from GD algorithm which requires *initialization at the origin* to reach the minimum-norm solution.

We study rPGD based on the intuition that  $\|w_t^\perp\|$  decreases after the normalization step. Hence,  $g_t w_t$  converges to a solution close to the minimum  $\ell_2$ -norm solution.

### 4.1. Orthogonal data matrix

We consider the simpler case when feature matrix  $A$  has orthonormal rows, i.e.,  $AA^\top = I$ , where  $I$  is an identity matrix. The algorithm rPGD follows two phases:

- **Phase I.** In the first  $T_1$  iterations, we either update only  $w$ , or both  $g, w$ . The orthogonal component  $w^\perp$  decreases geometrically, and it converges to the right direction  $w^*$ .
- **Phase II.** In the next  $T_2$  iterations, the algorithm updates  $w$  and  $g$  at the same time. The scale  $g$  increases and converges to the right scale  $g^*$ .

In both phases we update  $w$  with a special learning rate  $\eta_t = 1/g_t^2$ , which leads to significant simplifications. The choice of this learning rate is explained in detail in the proof. We have the following theorems, for the cases when  $g$  is updated or fixed in Phase I, respectively.

**Theorem 4.1** (Updating  $g$  in Phase I). *Suppose we initialize with  $g_0 < g^*$ . Let  $\delta_0 = (g^*)^2 - (g_0)^2 > 0$ . Suppose the number of iterations  $T_1$  and  $T_2$  is of the order:*

$$T_1 = \mathcal{O}\left(\frac{(g^*)^2}{\delta_0} \log\left(\frac{1}{\varepsilon}\right)\right),$$

$$T_2 = \mathcal{O}\left(\frac{1}{\gamma^{(2)}} \log\left(\frac{1}{\varepsilon}\right)\right).$$

For iterations  $t = 1, \dots, T_1 - 1$ , set the stepsize for  $g$  to<sup>1</sup>

$$\gamma^{(1)} \leq \min \left\{ \frac{g_0^2 \log\left(\frac{(g^*)^2}{2g_0^2} + \frac{1}{2}\right)}{2T_1((g^*)^2 - \|Ag_0w_0\|^2)}, \frac{1}{2(1 + \|Aw_0\|^2)} \right\}$$

and to any  $\gamma^{(2)} \leq \frac{1}{4}$  for  $t = T_1, T_1 + 1, \dots, T_1 + T_2 - 1$ . Set  $\eta_t = 1/g_t^2$  always. Then we reach  $\|w_T^\perp\|^2 \leq \varepsilon$  and  $\|Ag_Tw_T - b\| \leq \varepsilon$  after  $T = T_1 + T_2$  iterations.

We restate the theorem with the explicit forms of  $T_1$  and  $T_2$  including the proof in Appendix D. The theorem implies that rPGD with the *non-convex reparameterization* has linear convergence to the minimum-norm solution. The distance  $\delta_0$  plays a key role: the larger it is, the faster the linear convergence (i.e. smaller  $T_1$ ). Moreover, we show below that the algorithm finds the right direction even with fixed  $g$ . We find this interesting because it suggests that *one can update the scale more slowly and reap some benefits of regularization*.<sup>2</sup> See Figure 2 for detailed illustration.

**Theorem 4.2** (Fixing  $g$  in Phase I). *Suppose the initialization satisfies  $0 < g_0 < g^*$ , and that  $w_0$  is a random vector with  $\|w_0\| = 1$ . Set  $\eta_t = 1/g_t^2$  at all iterations. For any  $0 < \varepsilon < 0.5$ , suppose the learning rate of  $g$  in Phase II satisfies*

$$0 < \gamma < \frac{g^* - g_0}{(1 - \varepsilon^2)(g^* - g_0) + \varepsilon^2 g^*} < 1. \quad (12)$$

Let the number of iterations be

$$T_1 = \frac{\log(1/\varepsilon^2)}{\log(g^{*2}/g_0^2)}, \quad T_2 = \frac{\log\left(\frac{1 - (1 - \varepsilon^2)g_0/g^*}{\varepsilon^2}\right)}{\log\left(\frac{1}{1 - (1 - \varepsilon^2)\gamma}\right)}. \quad (13)$$

Then after  $T = T_1 + T_2$  iterations, the output of Algorithm 2 will satisfy

$$\langle w_T, w^* \rangle \geq 1 - \varepsilon, \quad (1 - 2\varepsilon^2)g^* \leq g_T \leq g^*, \quad (14)$$

<sup>1</sup>We let  $g_1 = g_0$  at the first step.

<sup>2</sup>This is different from (Kohler et al., 2019) using the optimal update for  $g$  in strongly convex setting.

which indicates that  $g_Tw_T$  is close to the minimum  $\ell_2$ -norm solution  $g^*w^*$ . We can also bound the final loss as  $f(w_T, g_T) = \|Ag_Tw_T - Ag^*w^*\|^2/2 \leq 3\varepsilon g^{*2}$ .

The proof with fixed  $g$  in Phase I is simpler, and can give some insight into the proof of 4.1. So we include the proof here.

*Proof.* For any vector  $w \in \mathbb{R}^d$ , we use  $w^\parallel \in \mathbb{R}^d$  to denote its projection onto the row space of  $A$ . We use  $w^\perp \in \mathbb{R}^d$  to denote its component in the subspace that is orthogonal to the row space of  $A$ . Since  $A$  has orthogonal rows, we can write  $w = w^\parallel + w^\perp$ , where

$$w^\parallel = A^\top Aw, \quad w^\perp = (I - A^\top A)w. \quad (15)$$

Since  $w^*$  is the minimum  $\ell_2$ -norm solution,  $w^{*\perp}$  must be zero, i.e.,  $(I - A^\top A)w^* = 0$  and  $A^\top Aw^* = w^*$ .

We will show that the algorithm has two phases. We now look at each phase in more detail.

**Phase I.** For any  $t = 0, \dots, T_1 - 1$ , only  $w$  is updated.

$$\begin{aligned} v_t &\stackrel{(a)}{=} w_t - \eta_t g_t^2 A^\top Aw_t + \eta_t g_t g^* A^\top Aw^* \\ &\stackrel{(b)}{=} (I - A^\top A)w_t + \frac{g^*}{g_0} A^\top Aw^* \\ &\stackrel{(c)}{=} w_t^\perp + \frac{g^*}{g_0} w^*, \end{aligned} \quad (16)$$

where (a) follows from substituting the partial gradient, (b) is true because of the choice of our learning rates:  $\eta_t = 1/g_t^2$  and  $\gamma_t = 0$ , and (c) follows from the fact that  $A$  has orthonormal rows. Since  $w_t^\perp$  is orthogonal to  $w^*$  and  $g_0 < g^*$ , we have

$$\|v_t\|^2 = \|w_t^\perp\|^2 + g^{*2}/g_0^2 \geq g^{*2}/g_0^2 > 1. \quad (17)$$

After normalization, we have  $w_{t+1} = v_t/\|v_t\|$ . As shown in equation 16, gradient update does not<sup>3</sup> change the component in the orthogonal subspace:  $v_t^\perp = w_t^\perp$ . Since  $\|v_t\|^2 > 1$ , the orthogonal component will shrink after the normalization step:

$$\|w_{t+1}^\perp\|^2 = \frac{\|v_t^\perp\|^2}{\|v_t\|^2} = \frac{\|w_t^\perp\|^2}{\|w_t^\perp\|^2 + g^{*2}/g_0^2} \leq \frac{g_0^2}{g^{*2}} \|w_t^\perp\|^2. \quad (18)$$

Since  $g_0 < g^*$ , after  $T_1 = \frac{\log(1/\varepsilon^2)}{\log(g^{*2}/g_0^2)}$  iterations, we have

$$\|w_{T_1}^\perp\|^2 \leq (g_0^2/g^{*2})^{T_1} \leq \varepsilon^2. \quad (19)$$

As indicated in (16),  $w_t^\parallel$  is in the same direction as  $w^*$  for  $t \geq 1$ . Since  $\|w_{T_1}^\perp\| \leq \varepsilon$ ,  $\|w_{T_1}^\parallel\| \geq \sqrt{1 - \varepsilon^2} \geq 1 - \varepsilon$ . Therefore,  $\langle w_{T_1}, w^* \rangle = \|w_{T_1}^\parallel\| \geq 1 - \varepsilon$ .

<sup>3</sup>This is always true for linear regression because the gradient  $\nabla_w f(w, g)$  lies in the row space of  $A$ .



**Phase II.** For iteration  $t = T_1, \dots, T_1 + T_2 - 1$ , the algorithm updates both  $w$  and  $g$ . The learning rate of updating  $g$  is set as a constant  $0 < \gamma < 1$ . The gradient update on  $g$  is

$$\begin{aligned} g_{t+1} &= g_t - \gamma g_t w_t^T A^\top A w_t + \gamma g^* w_t^T A^\top A w^* \\ &\stackrel{(a)}{=} g_t - \gamma g_t \|w_t^\parallel\|^2 + \gamma g^* \langle w_t^\parallel, w^* \rangle, \\ &\stackrel{(b)}{=} g_t - \gamma g_t \|w_t^\parallel\|^2 + \gamma g^* \|w_t^\parallel\|, \end{aligned} \quad (20)$$

where (a) follows from the fact that  $A$  has orthonormal rows and  $w^*$  lies in the row space of  $A$ , and (b) is true because (16) implies that  $w_t^\parallel$  is in the same direction as  $w^*$  for  $t \geq 1$ .

We will now prove that the following two properties (see Lemma E.7) hold during Phase II:

- Property (i):  $\|w_{t+1}^\perp\| \leq \|w_t^\perp\| \leq \varepsilon$ .
- Property (ii): letting  $\gamma' = \gamma(1 - \varepsilon^2)$ , we have

$$(1 - \gamma')g_t + \gamma'g^* \leq g_{t+1} \leq g^*.$$

We will now finish the proof of Theorem 4.2 using these two properties. After  $T = T_1 + T_2$  iterations, by Property (i) and the same argument as in Phase I, we have  $\langle w_T, w^* \rangle = \|w_T^\parallel\| \geq 1 - \varepsilon$ . By Property (ii), we can rewrite the lower bound of  $g_T$  as

$$\begin{aligned} g^* - g_T &\leq (1 - \gamma')(g^* - g_{T-1}) \\ &\leq (1 - \gamma')^{T_2}(g^* - g_{T_1}) \\ &\stackrel{(a)}{=} (1 - \gamma')^{T_2}(g^* - g_0) \\ &\stackrel{(b)}{\leq} 2\varepsilon^2 g^*, \end{aligned} \quad (21)$$

where (a) follows from the fact that  $g_{T_1} = g_0$ , and (b) follows from our choice of  $T_2$ : it is easy to verify that  $T_2$  satisfies  $(1 - \gamma')^{T_2}(g^* - g_0 + \delta) = \delta$ , which implies that  $(1 - \gamma')^{T_2}(g^* - g_0) < \delta$ . By our definition,  $\delta = \varepsilon^2 g^* / (1 - \varepsilon^2) < 2\varepsilon^2 g^*$  for  $0 < \varepsilon < 0.5$ . Therefore, by equation 21, we have  $g_T \geq (1 - 2\varepsilon^2)g^*$ .

Given  $\langle w_T, w^* \rangle \geq 1 - \varepsilon$  and  $(1 - 2\varepsilon^2)g^* \leq g_T \leq g^*$ , we can bound the loss as

$$\begin{aligned} f(w_T, g_T) &= g_T^2 \|Aw_T\|^2 / 2 - g_T g^* \langle Aw_T, Aw^* \rangle + g^{*2} / 2 \\ &\leq g^{*2} / 2 - (1 - 2\varepsilon^2)g^{*2}(1 - \varepsilon) + g^{*2} / 2 \\ &\leq 3\varepsilon g^{*2}. \end{aligned}$$

□

## 4.2. General data matrix

Inspired by the two-phase analysis for orthogonal  $A$ , we now extend it to a general matrix  $A$ . We analyze the following two phases for the optimization of general  $A$ :

- **Phase I.** In the first  $T_1$  iterations, we fix  $g := g_0$ , and update only  $w$  using rPGD. The orthogonal component  $w^\perp$  decreases geometrically such that  $\|w^\perp\| \leq \varepsilon$ .
- **Phase II.** In the next  $T_2$  iterations, we still keep  $g := g_0$  and update  $w$  using GD.

Phase I could be considered as finding a good initialization for Phase II. In Phase II, we use standard GD to converge to the final solution. Notice that  $\|w^\perp\|$  is invariant during gradient descent. Since  $\|w_{T_1}^\perp\| \leq \varepsilon$ , the final solution  $w_{T_1+T_2}$  still satisfies that  $\|w_{T_1+T_2}^\perp\| \leq \varepsilon$ . Because Phase II is linear regression with simple GD, the convergence is guaranteed and we omit this part of the analysis. We focus on the non-trivial case, Phase I.

The problem in Phase I is non-convex problem even with fixed  $g$  because the projection is on the sphere which is a non-convex object. However, suppose we can ensure that after each update, the gradient step  $v_t = w_t - \eta_t \nabla_w f(w_t, g_t)$  has larger than unit norm,  $\|v_t\| \geq 1$ . Then the constrained non-convex problem:

$$\min_{w \in \mathbb{R}^d} \|Ag_0 w - y\|^2 \text{ s.t. } w \in \{w, \|w\| = 1\}$$

is the same as the following convex problem:

$$\min_{w \in \mathbb{R}^d} \|Ag_0 w - y\|^2 \text{ s.t. } w \in \{w, \|w\| \leq 1\}.$$

This suggests that the analysis should simplify in this case, and we will see this in the argument.

**Theorem 4.3.** *For a full rank matrix  $A$  with  $\lambda_{\max}(AA^\top) = 1$ , we fix  $\delta > 0$ . In **Phase I** with fixed  $g$ , we can reach to a solution satisfying  $\|w_{T_1}^\perp\| \leq \varepsilon$  where*

$$T_1 = \frac{1}{\log(1 + \delta)} \log \left( \frac{\|w_0^\perp\|}{\varepsilon} \right)$$

if we set

$$g_0 \leq \frac{g^* \lambda_{\min}(AA^\top)}{2 + \delta}. \quad (22)$$

Moreover, if the singular values of  $A$  do not decrease too fast, so that the following inequality holds:

$$\frac{1}{m} \|AA^\top\|_F^2 \geq \lambda_{\min}^2(AA^\top) + 2\sqrt{\frac{\log(m)}{m}}, \quad (23)$$

and  $w^*$  is randomly drawn on the sphere, then with probability  $1 - \mathcal{O}(\frac{1}{m})$ , we only need that

$$g_0 \leq \frac{g^*}{(2 + \delta)} \sqrt{\frac{\|AA^\top\|_F^2 - 2\sqrt{m \log(m)}}{m}}. \quad (24)$$

The proof of Theorem 4.3 is in Appendix F. The theorem basically implies that if we set  $g_0$  satisfying inequality 22 for general  $A$  and  $w^*$  or inequality 24 for some particular  $A$  and  $w^*$ , running rPGD with fixed  $g_0$  helps with regularizing the iterates to converge to the minimum-norm solution.

## 5. Experiments

In this section, we evaluate WN and rPGD on two problems: linear regression and matrix sensing. We show that for a wide range of initialization, WN and rPGD converges to the minimum norm solution: it is the minimum  $\ell_2$ -norm solution for linear regression and the minimum nuclear norm solution for matrix sensing. This is in contrast to the standard gradient descent (GD) algorithm. For both problems GD requires initialization very close to, or exactly at, the origin to converge to the minimum norm solution (Li et al., 2018). We will mainly compare with the following two step-size schemes.

- $\gamma_t = \eta_t$ : We simultaneously update the weight vector (matrix) and the scalar  $g$ . This is similar to the training of deep neural networks, where we use the same learning rate for all of the layers.
- Two-phase algorithm: In **Phase I**, we only update the direction component (weight vector in linear regression and weight matrix in matrix sensing), while in **Phase II**, we update both the scale component (a scalar in linear regression and a scalar / matrix in matrix sensing, see below) and the direction component.

### 5.1. Linear Regression

Let  $m = 20$ ,  $d = 50$ . We generate the feature matrix as  $A = U\Sigma V^T \in \mathbb{R}^{m \times d}$ , where  $U \in \mathbb{R}^{m \times m}$  and  $V \in \mathbb{R}^{d \times m}$  are two random orthogonal matrices chosen uniformly over the Stiefel manifold of partial orthogonal matrices, and  $\Sigma$  is a diagonal matrix described below.

Let  $\kappa = \frac{\lambda_{\max}(AA^\top)}{\lambda_{\min}(AA^\top)}$ . We will vary the condition number  $\kappa \geq 1$  of  $A$  in our experiments. The diagonal entries of  $\Sigma$  are set as  $1, (1/\kappa)^{1/(m-1)}, (1/\kappa)^{2/(m-1)}, \dots, 1/\kappa$ . The maximum eigenvalue of  $A^\top A$  is  $\lambda_{\max} = 1$ . Set  $g^* = 3$ , and  $w^*$  as an arbitrary unit norm vector in the row space of  $A$ .

**Orthogonal A.** Let  $w_0$  be a random unit norm vector. We run the standard gradient descent (GD) algorithm on the linear regression problem  $f(x) = \|Ax - y\|_2^2/2$  starting from the initialization point  $x_0 = g_0 w_0$ . We run Algorithm 1 and 2 starting from the same initialization, and plot  $|\hat{g}| = \|\hat{g}\hat{w}\|_2$  as a function of  $g_0$ . We run all of the algorithms until the squared loss satisfies  $f(\hat{w}, \hat{g}) \leq 10^{-5}$ ,

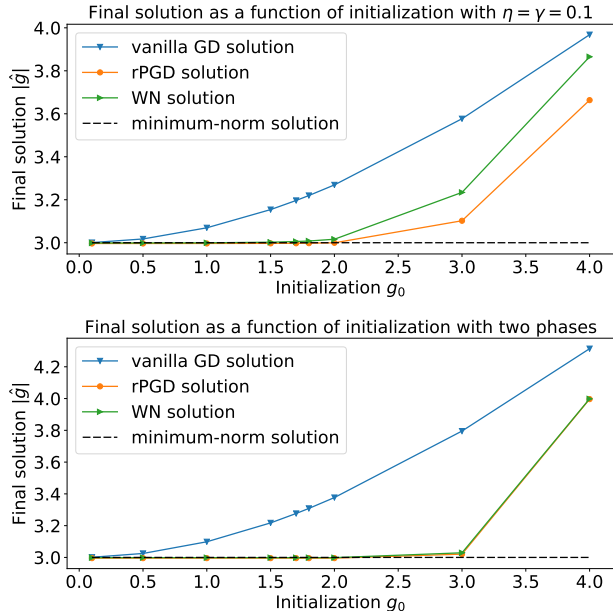


Figure 4: Comparison of the final solutions  $|\hat{g}| = \|\hat{g}\hat{w}\| = \|\hat{x}\|$  provided by GD, WN and our proposed rPGD on an overparameterized linear regression problem  $\min_x \frac{1}{2} \|Ax - y\|_2^2$ . All algorithms start from the same initialization  $x_0 = g_0 w_0$ . Compared to GD, WN and rPGD converge to the minimum  $\ell_2$ -norm solution for a larger region of initialization. Top plot is when we use the same stepsize for  $w$  and  $g$ :  $\gamma_t = \eta_t = 0.1$ . Bottom plot is when we use a particularly small stepsize for  $g$  and optimal stepsize for  $w$ . This implies that a small stepsize for  $g$  can arrive to a solution that is close to the minimum-norm solution for even wider range of  $g_0$ . The green, orange and black curves overlap in both plots when  $0 \leq g_0 \leq 2$ .

where the final solution is denoted as  $\hat{g}\hat{w}$ . We have the following observations:

- **Figure 1** shows the result when we set a very small but equal learning rate for  $w$  and  $g$ :  $\eta_t = \gamma_t = 0.005$ . It shows there is no difference between WN and rPGD when the learning rate is small, which matches Lemma 3.1. We can see that both WN and rPGD can get close to the minimum-norm solution with a large range of initializations ( $g^* w^*$  for  $g_0 \lesssim 1.5$ ) while this is only true for GD when  $g_0$  is close to 0. This experiment provides support to our theory.
- **The top plot in Figure 4** shows the result when we set relatively large learning rates of  $w$  and  $g$ :  $\eta_t = \gamma_t = 0.1$ , as in practice where we use the same non-vanishing learning rate for all the layers when training deep neural networks. The plot shows a difference between WN and rPGD when  $g_0 > 2$  when we use

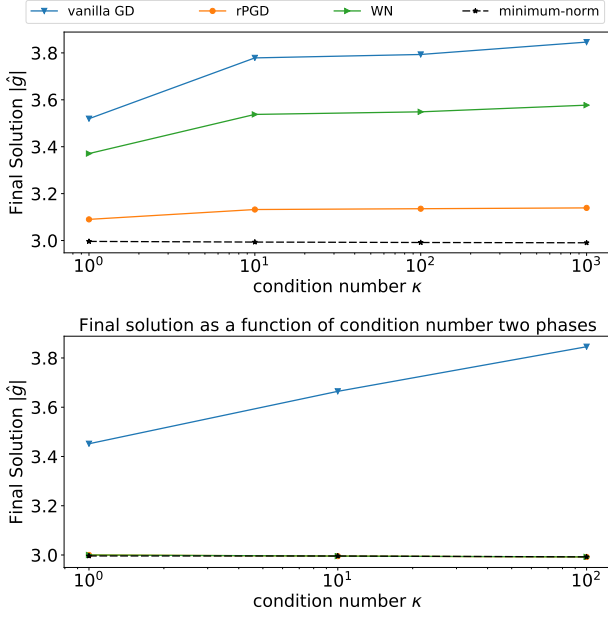


Figure 5: Fix  $g_0 = 2.8$  and increase the condition number  $\kappa$ . Top plot:  $\gamma_t = \eta_t = 0.01$ . The  $\ell_2$ -norm of the WN and rPGD solutions increases slowly as  $\kappa$  increases, but their norm is smaller than when using Gradient Descent. Bottom plot:  $\gamma_t = 1, \eta_t = 0.1 \times \mathbb{1}_{\{t > 5000\}}$ . The  $\ell_2$ -norm of WN and rPGD solutions are robust to condition number and close to the minimum  $\ell_2$ -norm for any  $\kappa$ . Note that green, orange and black curves of the bottom plot overlap.

large learning rates. However, there is not too much difference between WN and rPGD when  $g_0 < 2$ .

- **The bottom plot in Figure 4** is when we set (1) WN  $\eta_t = \|w_t\| / (g_t^2 \lambda_{\max})$  for  $w$  and  $\gamma_t = 0.005$  for  $g$ ; (2) rPGD  $\eta_t = 1 / (g_t^2 \lambda_{\max})$  and  $\gamma_t = 0.005$ . This mimics the two-phase algorithm as shown in Theorem 4.1. We can arrive at a solution close to the minimum-norm solution for even wider range of  $g_0 \lesssim 3$ .

**Robustness to the condition number  $\kappa$ .** We repeat the previous experiment for various input matrix  $A$  with a wider range of  $\kappa$ . We set the initialization  $g_0$  as 2.8. The results are shown in Figure 5. We see that for  $\gamma_t = \eta_t$  (the top plot in Figure 5) as  $\kappa$  increases, the  $\ell_2$ -norm of the solutions provided by WN and rPGD also gradually increases but not as much as those provided by the vanilla GD. The bottom plot in Figure 5 shows that the performance of the two-phase algorithms, with  $\eta_t = 0$  in the first 5000 iterations, thus have a better performance compared with one-phase algorithm shown in the top plot in Figure 5. This is even though the one-phase algorithm has relatively small learning rate compared with the two-phase algorithm.

## 5.2. Matrix Sensing

We show that the normalization methods can also be applied to the matrix sensing problem, to get closer to the minimum nuclear norm solutions. The goal in the matrix sensing problem is to recover a low-rank matrix from a small number of random linear measurements. Here we follow the setup considered in Li et al. (2018) (for more related work on matrix sensing and completion, see, e.g., (Candès and Recht, 2009; Donoho et al., 2013; Ge et al., 2016) and references therein). Let  $X^* = U^*U^{*T} \in \mathbb{R}^{d \times d}$  (with  $U^* \in \mathbb{R}^{d \times r}$ ) be the ground-truth rank- $r$  matrix. Let  $A_1, \dots, A_m \in \mathbb{R}^{d \times d}$  be  $m$  random sensing matrices, with each entry sampled from a standard Gaussian distribution. We are interested in the setting when  $r \ll d$  and  $m \ll d^2$ . Given  $m$  linear measurements of the form  $\langle A_i, X^* \rangle$ , let  $U \in \mathbb{R}^{d \times d}$  be the variable matrix, we define the (over-parameterized) loss function as

$$f(U) = \frac{1}{2m} \sum_{i=1}^m (\langle A_i, UU^T \rangle - \langle A_i, X^* \rangle)^2. \quad (25)$$

It is proved in (Li et al., 2018) that if  $m = \tilde{O}(dr^2)$ , then gradient descent on  $f(U)$ , when initialized very close to the origin, can recover the low-rank matrix  $X^*$ .

**WN.** To apply WN, we need to reparametrize  $U$  into a direction variable and a scale variable. We consider two choices:

- Let  $UU^T = g \frac{WW^T}{\|W\|_F^2}$ , where  $g \in \mathbb{R}$ , and  $W \in \mathbb{R}^{d \times d}$ . In Figure 6, the green curve represents this algorithm. We label it with **WN**.
- Let  $UU^T = WDW^T$ , where  $D \in \mathbb{R}^{d \times d}$  is a diagonal matrix, and all the column vectors of  $W \in \mathbb{R}^{d \times d}$  have unit  $\ell_2$  norm. That is, for  $w_i \in \mathbb{R}^d, i = 1, 2, \dots, d$

$$W = \begin{bmatrix} \frac{w_1}{\|w_1\|} & \frac{w_2}{\|w_2\|} & \dots & \frac{w_d}{\|w_d\|} \end{bmatrix}.$$

In Figure 6, the purple curve represents the algorithm. We label it with **WN-Diag** where ‘‘Diag’’ references the diagonal matrix.

**rPGD.** To apply rPGD, we need to reparametrize  $U$  into a direction variable and a scale variable. We consider two choices:

- Let  $UU^T = gWW^T$ , where  $g \in \mathbb{R}$ , and  $W \in \mathbb{R}^{d \times d}$  satisfies  $\|W\|_F = 1$ . See Algorithm 3. In Figure 6, the orange curve represents the algorithm. We label it with **rPGD**.
- Let  $UU^T = WDW^T$ , where  $D \in \mathbb{R}^{d \times d}$  is a diagonal matrix, and all the column vectors of  $W \in \mathbb{R}^{d \times d}$  are

projected to have unit  $\ell_2$  norm. See Algorithm 4. In Figure 6, the red curve represents the algorithm. We label it with **rPGD-Diag**.

---

**Algorithm 3 rPGD** for matrix sensing loss  $f(W, g)$

---

**Input:** initialization  $W_0$  and  $g_0$ , number of iterations  $T$ , step-sizes  $\gamma_t$  and  $\eta_t$ .  
**for**  $t = 0, 1, 2, \dots, T - 1$  **do**  
 $V_t = W_t - \eta_t \nabla_W f(W_t, g_t)$   
 $W_{t+1} = \frac{V_t}{\|V_t\|_F}$   
 $g_{t+1} = g_t - \gamma_t \nabla_g f(W_t, g_t)$   
**end for**

---



---

**Algorithm 4 rPGD-Diag** for matrix sensing loss  $f(W, D)$

---

**Input:** initialization  $W_0$  and  $D_0$ , number of iterations  $T$ , step-sizes  $\gamma_t$  and  $\eta_t$ .  
**for**  $t = 0, 1, 2, \dots, T - 1$  **do**  
 $V_t = W_t - \eta_t \nabla_W f(W_t, D_t)$   
 $W_{t+1} = V_t$  with all column vectors normalized.  
 $\text{diag}(D_{t+1}) = \text{diag}(D_t) - \gamma_t \text{diag}(\nabla_D f(W_t, D_t))$   
**end for**

---

Denote the corresponding loss functions for rPGD as  $f(W, g)$  and  $f(W, D)$ . Let  $Z$  be a matrix with i.i.d. Gaussian entries, after which all column vectors have been normalized. We set the experiments with the following initialization:

- For vanilla GD on  $f(U)$ , let  $U_0 = \alpha Z$ ;
- For WN and rPGD, let  $W_0 = \frac{Z}{\|Z\|_F}$  so that  $\|W_0\|_F = 1$ , and  $g_0 = \alpha^2 \|Z\|_F$ ;
- For WN-Diag and rPGD-Diag, let  $W_0 = Z$  and  $D_0 = \alpha^2 I$ .

We set  $d = 30$ ,  $r = 4$ , and  $m = 60$ . We simulate  $y_i = \langle A_i, \hat{U}\hat{U} \rangle$  with  $\hat{U} \in \mathbb{R}^{d \times r}$  generated as a random matrix.<sup>4</sup>

We compare the performance of gradient descent, and our algorithms for several initializations scales  $g$ . We run each algorithm until convergence (i.e., when the squared loss is less than  $10^{-6}$ ).

Similar to Figure 3, we use different learning rate schemes to get the final solution. We use grid search to find appropriate constant learning rate  $c$ .<sup>5</sup> The top plot in Figure 6

<sup>4</sup>Code:  $\hat{U} = \text{numpy.random.randn}(d, r)$ . Note that this is not necessary the minimum nuclear solution. We use the python package ‘‘cvxpy’’ to solve for the minimum nuclear solution for equation 25.

<sup>5</sup>Note  $c$  varies for different  $g_0$  and different algorithms. Here we start with 0.5 and then decay by a factor of 2 until we get a step-size that can converge to the solution.

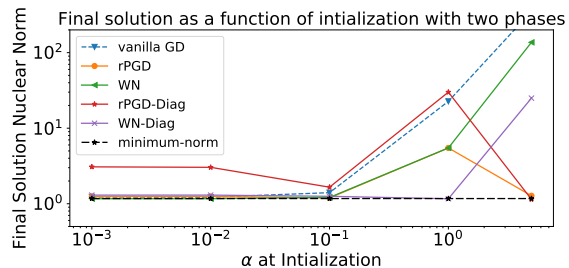
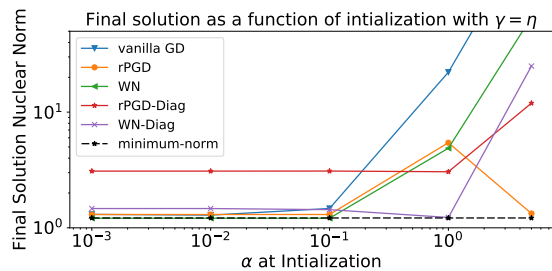


Figure 6: Comparison of the final solutions  $\|\hat{X}\|_*$  provided by GD, WN, and rPGD on an overparameterized matrix sensing problem (equation 25). All algorithms start from the same initialization with the scale  $\alpha = \sqrt{\|UU^T\|_F}$ . Compared to GD, WN and rPGD converge close to the minimum nuclear-norm solution for a broader region of initialization. The top plot is when we use the same stepsize for  $W$  and  $g$ :  $\gamma_t = \eta_t = c$ . The bottom plot is when we use  $\eta_t = c$  and  $\gamma_t = c\mathbb{1}_{\{t > 1000\}}$ . This suggests that Two-phase algorithm can arrive to a solution closer to the nuclear-norm solution for a broader range of  $g_0$ . The blue, green, and black curves of the top plot overlap when  $0 < \alpha < 0.1$ . The blue, orange, green, purple, and black curves of the bottom plot overlap when  $0 < \alpha < 0.1$ .

uses the following learning rate: constant  $c$  for gradient descent;  $\eta_t = \gamma_t = c$  for rPGD (Algorithm 3 and 4); and set  $\eta_t = \gamma_t = c\|W\|_F$  for WN. The bottom plot in Figure 6 uses the two phase learning rates: constant for gradient descent;  $\eta_t = c$  and  $\gamma_t = c\mathbb{1}_{\{t > 1000\}}$  for rPGD (Algorithm 3 and 4); and set  $\eta_t = \gamma_t = c\|W\|_F$  and  $\gamma_t = c\mathbb{1}_{\{t > 1000\}}$  for WN. Compared to GD, WN and rPGD converge close to the minimum nuclear-norm solution for a larger region of initialization. Moreover, these results also suggest that with the two-phase algorithm, one can arrive to a solution close to the nuclear-norm solution for a wider range of  $g_0$ .

## Acknowledgments

XW, ED, SG, and RW thank the Institute for Advanced Study for their hospitality during the Special Year on Optimization, Statistics, and Theoretical Machine Learning. XW, SW, ED, SG, and RW thank the Simons Institute for

their hospitality during the Summer 2019 program on the Foundations of Deep Learning. RW acknowledges funding from AFOSR and Facebook AI Research. This material is based upon work supported by the National Science Foundation under Grant No. DMS-1638352.

## References

- Alnur Ali, J Zico Kolter, and Ryan J Tibshirani. A continuous-time view of early stopping for least squares regression. *arXiv preprint arXiv:1810.10082*, 2018.
- Sanjeev Arora, Zhiyuan Li, and Kaifeng Lyu. Theoretical analysis of auto rate-tuning by batch normalization. *arXiv preprint arXiv:1812.03981*, 2018.
- Sanjeev Arora, Nadav Cohen, Wei Hu, and Yuping Luo. Implicit regularization in deep matrix factorization. *arXiv preprint arXiv:1905.13655*, 2019.
- Jimmy Lei Ba, Jamie Ryan Kiros, and Geoffrey E Hinton. Layer normalization. *arXiv preprint arXiv:1607.06450*, 2016.
- Peter L Bartlett, Philip M Long, Gábor Lugosi, and Alexander Tsigler. Benign overfitting in linear regression. *arXiv preprint arXiv:1906.11300*, 2019.
- Mikhail Belkin, Daniel Hsu, and Ji Xu. Two models of double descent for weak features. *arXiv preprint arXiv:1903.07571*, 2019.
- Yongqiang Cai, Qianxiao Li, and Zuowei Shen. A quantitative analysis of the effect of batch normalization on gradient descent. In *International Conference on Machine Learning*, pages 882–890, 2019.
- Emmanuel J Candès and Benjamin Recht. Exact matrix completion via convex optimization. *Foundations of Computational mathematics*, 9(6):717, 2009.
- Shuxiao Chen, Edgar Dobriban, and Jane H Lee. Invariance reduces variance: Understanding data augmentation in deep learning and beyond. *arXiv preprint arXiv:1907.10905*, 2019.
- Edgar Dobriban and Stefan Wager. High-dimensional asymptotics of prediction: Ridge regression and classification. *The Annals of Statistics*, 46(1):247–279, 2018.
- David L Donoho, Matan Gavish, and Andrea Montanari. The phase transition of matrix recovery from gaussian measurements matches the minimax mse of matrix denoising. *Proceedings of the National Academy of Sciences*, 110(21):8405–8410, 2013.
- Scott C Douglas, Shun-ichi Amari, and S-Y Kung. On gradient adaptation with unit-norm constraints. *IEEE Transactions on Signal Processing*, 48(6):1843–1847, 2000.
- Simon S Du, Jason D Lee, Yuandong Tian, Aarti Singh, and Barnabas Poczos. Gradient descent learns one-hidden-layer cnn: Dont be afraid of spurious local minima. In *International Conference on Machine Learning*, pages 1338–1347, 2018.
- Rong Ge, Jason D Lee, and Tengyu Ma. Matrix completion has no spurious local minimum. In *Advances in Neural Information Processing Systems*, pages 2973–2981, 2016.
- David Gleich and Michael Mahoney. Anti-differentiating approximation algorithms: A case study with min-cuts, spectral, and flow. In *International Conference on Machine Learning*, pages 1018–1025, 2014.
- Suriya Gunasekar, Blake E Woodworth, Srinadh Bhojanapalli, Behnam Neyshabur, and Nati Srebro. Implicit regularization in matrix factorization. In *Advances in Neural Information Processing Systems*, pages 6151–6159, 2017.
- Suriya Gunasekar, Jason Lee, Daniel Soudry, and Nathan Srebro. Characterizing implicit bias in terms of optimization geometry. *arXiv preprint arXiv:1802.08246*, 2018.
- Trevor Hastie, Andrea Montanari, Saharon Rosset, and Ryan J Tibshirani. Surprises in high-dimensional ridgeless least squares interpolation. *arXiv preprint arXiv:1903.08560*, 2019.
- Uwe Helmke and John B Moore. *Optimization and dynamical systems*. Springer Science & Business Media, 2012.
- Elad Hoffer, Ron Banner, Itay Golan, and Daniel Soudry. Norm matters: efficient and accurate normalization schemes in deep networks. In *Advances in Neural Information Processing Systems*, pages 2160–2170, 2018.
- Sergey Ioffe and Christian Szegedy. Batch normalization: Accelerating deep network training by reducing internal covariate shift. *arXiv preprint arXiv:1502.03167*, 2015.
- Ziwei Ji and Matus Telgarsky. The implicit bias of gradient descent on nonseparable data. In *Conference on Learning Theory*, pages 1772–1798, 2019.
- Jonas Kohler, Hadi Daneshmand, Aurelien Lucchi, Thomas Hofmann, Ming Zhou, and Klaus Neymeyr. Exponential convergence rates for batch normalization: The power of length-direction decoupling in non-convex optimization. In *AISTATS*, pages 806–815, 2019.
- Qi Lei, Ian EH Yen, Chao-yuan Wu, Inderjit S Dhillon, and Pradeep Ravikumar. Doubly greedy primal-dual coordinate descent for sparse empirical risk minimization. In *Proceedings of the 34th International Conference on Machine Learning-Volume 70*, pages 2034–2042, 2017.

- Yuanzhi Li, Tengyu Ma, and Hongyang Zhang. Algorithmic regularization in over-parameterized matrix sensing and neural networks with quadratic activations. In *Conference On Learning Theory*, 2018.
- Xiangru Lian and Ji Liu. Revisit batch normalization: New understanding and refinement via composition optimization. In Kamalika Chaudhuri and Masashi Sugiyama, editors, *Proceedings of Machine Learning Research*, volume 89 of *Proceedings of Machine Learning Research*, pages 3254–3263, 16–18 Apr 2019.
- Tengyuan Liang and Alexander Rakhlin. Just interpolate: Kernel "ridgeless" regression can generalize. *arXiv preprint arXiv:1808.00387*, 2018.
- Sifan Liu and Edgar Dobriban. Ridge regression: Structure, cross-validation, and sketching. *arXiv preprint arXiv:1910.02373*, 2019.
- Ping Luo, Xinjiang Wang, Wenqi Shao, and Zhanglin Peng. Towards understanding regularization in batch normalization. In *International Conference on Learning Representations*, 2019.
- Michael Mahoney and Charles Martin. Traditional and heavy tailed self regularization in neural network models. In *International Conference on Machine Learning*, pages 4284–4293, 2019.
- Michael W Mahoney. Approximate computation and implicit regularization for very large-scale data analysis. In *Proceedings of the 31st ACM SIGMOD-SIGACT-SIGAI symposium on Principles of Database Systems*, pages 143–154. ACM, 2012.
- Michael W Mahoney and Lorenzo Orecchia. Implementing regularization implicitly via approximate eigenvector computation. In *Proceedings of the 28th International Conference on International Conference on Machine Learning*, pages 121–128. Omnipress, 2011.
- Charles H Martin and Michael W Mahoney. Implicit self-regularization in deep neural networks: Evidence from random matrix theory and implications for learning. *arXiv preprint arXiv:1810.01075*, 2018.
- Nelson Morgan and Hervé Bouchard. Generalization and parameter estimation in feedforward nets: Some experiments. In *Advances in neural information processing systems*, pages 630–637, 1990.
- Behnam Neyshabur, Ryota Tomioka, and Nathan Srebro. In search of the real inductive bias: On the role of implicit regularization in deep learning. *arXiv preprint arXiv:1412.6614*, 2014.
- Tomaso Poggio, Andrzej Banburski, and Qianli Liao. Theoretical issues in deep networks: Approximation, optimization and generalization. *arXiv preprint arXiv:1908.09375*, 2019.
- Tim Salimans and Diederik P Kingma. Weight normalization: A simple reparameterization to accelerate training of deep neural networks. In *Advances in Neural Information Processing Systems*, pages 901–909, 2016.
- Shibani Santurkar, Dimitris Tsipras, Andrew Ilyas, and Aleksander Madry. How does batch normalization help optimization? In *Advances in Neural Information Processing Systems*, pages 2483–2493, 2018.
- Daniel Soudry, Elad Hoffer, Mor Shpigel Nacson, Suriya Gunasekar, and Nathan Srebro. The implicit bias of gradient descent on separable data. *The Journal of Machine Learning Research*, 19(1):2822–2878, 2018.
- Otto Neall Strand. Theory and methods related to the singular-function expansion and landwebers iteration for integral equations of the first kind. *SIAM Journal on Numerical Analysis*, 11(4):798–825, 1974.
- Yuangong Tian. Over-parameterization as a catalyst for better generalization of deep relu network. *arXiv preprint arXiv:1909.13458*, 2019.
- Yuangong Tian, Tina Jiang, Qucheng Gong, and Ari Morcos. Luck matters: Understanding training dynamics of deep relu networks. *arXiv preprint arXiv:1905.13405*, 2019.
- Tomas Vaškevičius, Varun Kanade, and Patrick Rebeschini. Implicit regularization for optimal sparse recovery. *arXiv preprint arXiv:1909.05122*, 2019.
- Roman Vershynin. *High-dimensional probability: An introduction with applications in data science*, volume 47. Cambridge University Press, 2018.
- Stefan Wager, Sida Wang, and Percy S Liang. Dropout training as adaptive regularization. In *Advances in neural information processing systems*, pages 351–359, 2013.
- Rachel Ward, Xiaoxia Wu, and Leon Bottou. AdaGrad stepsizes: Sharp convergence over nonconvex landscapes. In *Proceedings of the 36th International Conference on Machine Learning*, pages 6677–6686, 09–15 Jun 2019.
- Xiaoxia Wu, Rachel Ward, and Léon Bottou. Wngrad: learn the learning rate in gradient descent. *arXiv preprint arXiv:1803.02865*, 2018.

## A. Proof of Lemma 3.1

*Proof. rPGD.* First, the gradient step on  $g$  clearly leads to the gradient flow for  $g$ . Second, for the update on  $w$ , we expand all terms to first order in  $\eta$ . Let  $a_t = \nabla_{w_t} f(w_t, g_t)$ :

$$\begin{aligned} w_{t+1} &= \frac{w_t - \eta \nabla_{w_t} f(w_t, g_t)}{\|w_t - \eta \nabla_{w_t} f(w_t, g_t)\|_2} \\ &= \frac{w_t - \eta a_t}{1 - \eta w_t^\top a_t + O(\eta^2)} \\ &= (w_t - \eta a_t) \cdot (1 + \eta w_t^\top a_t + O(\eta^2)) \\ &= w_t - \eta a_t + \eta w_t w_t^\top a_t + O(\eta^2) \\ &= w_t - \eta P_{w_t^\perp} a_t + O(\eta^2). \end{aligned}$$

Taking  $\eta \rightarrow 0$ , we obtain the WN flow dynamics.

**WN.** We now study weight normalization (Salimans and Kingma, 2016). The WN objective function can be written as

$$h(g, w) = \frac{1}{2} \left\| y - g \frac{Aw}{\|w\|} \right\|_2^2.$$

We train this "backpropagating" on  $g, w$ , i.e., by gradient descent on both parameters. Let  $r$  be the negative residual as before. Recall that the gradients of  $f(g, w) = \|y - Agw\|^2/2$  are

$$\nabla_w f(w, g) = g A^T r, \quad \nabla_g f(w, g) = w^T A^T r.$$

Now

$$\begin{aligned} \nabla_g h(w, g) &= r^T \frac{Aw}{\|w\|} \\ \nabla_w h(w, g) &= g [J_w \frac{Aw}{\|w\|}]^T r \\ &= g \left( I - \frac{ww^T}{\|w\|^2} \right) A^T \frac{r}{\|w\|}. \end{aligned}$$

The discrete time algorithm is thus updated as

$$\begin{aligned} v_t &= w_t / \|w_t\| \\ r_t &= y - g_t A v_t \\ g_{t+1} &= g_t - \eta \cdot r_t^T A v_t \\ w_{t+1} &= w_t - \eta \cdot g_t \cdot P_{w_t^\perp} \frac{A^T r_t}{\|w_t\|}. \end{aligned}$$

When  $\eta \rightarrow 0$ , we recover the gradient flow on  $g_t$ , i.e.,

$$\dot{g}_t = -r_t^T A v_t.$$

Moreover, for  $w_t$ , we find

$$\dot{w}_t = -g_t \cdot P_{w_t^\perp} \frac{A^T r_t}{\|w_t\|}.$$

Since  $w_t^T \dot{w}_t = 0$ , we have that  $\|w_t\|$  is constant (This has been found in (Tian et al., 2019; Tian, 2019)). Hence, we have that  $g_t, v_t$  evolves exactly according to the WN flow:

$$\begin{aligned} \dot{g}_t &= -r_t^T A v_t \\ \dot{v}_t &= -g_t \cdot P_{w_t^\perp} A^T r_t. \end{aligned}$$

□

## B. Proof of Theorem 3.2

*Proof.* The proof proceeds by calculating the derivatives of several quantities systematically, and noticing some unexpected invariants.

### B.1. Part I

Let  $w^\perp = P^\perp w$ , where  $P^\perp$  is the projection into the orthocomplement of the row span of  $A$ , and hence  $P^\perp A^T = 0$ .

For simplicity, write  $L(x_t) = L_t = \|Ax_t - b\|^2/2$  with  $x_t = g_t \frac{w_t}{\|w_t\|}$ . Let  $\nabla L_t = A^\top r_t$  where  $r_t = Ax_t - b$ . In the next calculation, we do not assume  $\|w_0\| = 1$ , but instead allow it to be arbitrary. Then we can calculate

$$\begin{aligned} \frac{dw_t^\perp}{dt} &= P^\perp \frac{dw_t}{dt} = -\frac{g_t}{\|w_t\|} P^\perp \left( I - \frac{w_t w_t^\top}{\|w_t\|^2} \right) \nabla L_t = \frac{g_t}{\|w_t\|} P^\perp \frac{w_t w_t^\top}{\|w_t\|^2} \nabla L_t = \frac{g_t}{\|w_t\|^2} P^\perp w_t \nabla_g h(g_t, w_t) \\ &= -\frac{g_t}{\|w_t\|^2} P^\perp w_t \dot{g}_t = -\frac{1}{2} \frac{P^\perp w_t}{\|w_t\|^2} \frac{dg_t^2}{dt} = -\frac{1}{2} \frac{w_t^\perp}{\|w_0\|^2} \frac{dg_t^2}{dt} = -k_0 w_t^\perp \frac{dg_t^2}{dt}. \end{aligned}$$

where  $k_0 = \frac{1}{2\|w_0\|^2}$ . Thus we have

$$w^\perp = \exp\left(\frac{g_0^2 - g^2}{2\|w_0\|^2}\right) w_0^\perp.$$

Since we initialize  $\|w_0\| = 1$ . We have the equation 10 in the theorem.

Now we look at the convergence of the dynamics, by calculating the derivative of the loss:

$$\begin{aligned} d[1/2 \cdot \|r_t\|^2]/dt &= r_t^\top \dot{r}_t = r_t^\top Ad(g_t w_t)/dt \\ &= r_t^\top A[\dot{g}_t w_t + g_t \dot{w}_t] \\ &= -r_t^\top A[w_t w_t^\top A^\top r_t + g_t^2 P_{w_t^\perp} A^\top r_t] \\ &= -r_t^\top A[w_t w_t^\top + g_t^2 P_{w_t^\perp}] A^\top r_t. \end{aligned}$$

Thus, we get a geometric convergence of the loss to zero, as soon as we can get a lower bound on  $g_t^2$ . In more detail, suppose we have  $g_t^2 \geq c$  for some constant  $c > 0$ . Then, we have

$$\begin{aligned} r_t^\top A[w_t w_t^\top + g_t^2 P_{w_t^\perp}] A^\top r_t &\geq r_t^\top A[w_t w_t^\top + c P_{w_t^\perp}] A^\top r_t \\ &\geq \min(c, 1) r_t^\top A A^\top r_t \\ &\geq \min(c, 1) \lambda_{\min}(A A^\top) \|r_t\|^2 \end{aligned}$$

and so with  $C := \min(c, 1) \lambda_{\min}(A A^\top)$ ,

$$d[1/2 \cdot \|r_t\|^2]/dt \leq -C \|r_t\|^2.$$

This implies that, as desired,

$$\|r_t\|^2 \leq \exp(-Ct) \|r_0\|^2.$$

Now,  $\|w_t^\perp\| \leq \|w_t\| = 1$ , hence we get the lower bound  $g_t^2 \geq 2 \log \|w_0^\perp\| + g_0^2 > 0$ . This shows that the loss converges to zero, finishing the proof for the general dynamics.

### B.2. Part II and III

For the fixed  $g_t$  case, we have

$$\begin{aligned} d[1/2 \cdot \|r_t\|^2]/dt &= r_t^\top \dot{r}_t = r_t^\top Ad(g_t w_t)/dt \\ &= r_t^\top A[\dot{g}_t w_t + g_t \dot{w}_t] \\ &= r_t^\top A g_0 \dot{w}_t \\ &= -r_t^\top A g_0 P_{w_t^\perp} g_0 A^\top r_t \\ &= -g_0^2 \|P_{w_t^\perp} A^\top r_t\|^2. \end{aligned}$$



Now, it follows that  $\|r_t\|$  is a non-increasing quantity, which is also strictly decreasing as long as  $\|P_{w_t^\perp} A^T r_t\| > 0$ . It also follows that as  $t \rightarrow \infty$ , we have  $\|P_{w_t^\perp} A^T r_t\| \rightarrow 0$ . Now, since  $g_0 < g^*$ , it follows that  $A^T r_t$  has a norm that is strictly bounded away from zero, i.e.,  $\|A^T r_t\| > c_0 > 0$  for some  $c_0 > 0$ . So, we do not have the residual going to zero in this case. Hence, this can also be written as  $w_t = c_t \cdot A^T r_t / \|A^T r_t\|$ , for some sequence of scalars  $c_t$  with  $\liminf c_t^2 > 0$ .

Hence,  $w_t$  becomes asymptotically parallel to the row space of  $A$ . Now, since  $w_t$  lives on the compact space of unit vectors, considering any subsequence of it, it also follows that it has a convergent subsequence. Let  $w$  be the limit along any convergent subsequence. It follows that  $w = \pm A^T r / \|A^T r\|$ . Next we note that the solution with  $+$  actually *maximizes* the loss over  $\|w\| = 1$ . Hence, the only possible solution is  $w = -A^T r / \|A^T r\|$ . Since this holds for any convergent subsequence, it follows that  $w_t$  itself must converge.

Now we get a more explicit form for the solution  $w$ . We can say that  $w$  is the unique unit norm vector such that  $w = -cA^T r$ , for some  $c > 0$ . Then we can write that equation as

$$\begin{aligned} w &= -cA^T (Agw - y) \\ (I + cgA^T A)w &= cA^T y \\ w &= (c^{-1}I + gA^T A)^{-1} A^T y. \end{aligned}$$

Thus,  $w$  is the unique vector of the above form such that  $\|w\| = 1$ . This can be viewed as a form of implicit regularization. Namely,  $w$  is the unique vector, for which there is some regularization parameter  $c$  such that,  $w$  minimizes the regularized least squares objective

$$\frac{1}{2} \|Agw - y\|^2 + \frac{g}{2c} \|w\|^2$$

and  $\|w\| = 1$ . This  $w$  will in general not be pointing in the direction of the optimal solution. We recall that the optimal solution  $w^*$  has the form  $w^* = A^\dagger b / \|A^\dagger b\|$ , where  $A^\dagger$  is the pseudoinverse of  $A$ . We recall that the action of the pseudoinverse can be characterized as the limit of ridge regularization with infinitely small penalization, i.e.,  $A^\dagger y = \lim_{\lambda \rightarrow 0} (A^T A + \lambda I)^{-1} A^T y$ . For orthogonal  $A$ , we see that  $w$  converges to the right direction, because  $A^T = A^\dagger$ . However, for general  $A$ , the flow does not in general converge to the min-norm direction.

Now, suppose we start the flow for both  $g_t, w_t$  again from a point  $w_0$  that belongs to the span of the row space of  $A$  (call it  $R$ ). Then, by the update rule for  $w_t$ , it follows that  $w_t \in R$  for all  $t$ . Therefore, the derivative of the loss becomes

$$\begin{aligned} d[1/2 \cdot \|r_t\|^2]/dt &= r_t^T \dot{r}_t = r_t^T A d(g_t w_t)/dt \\ &= r_t^T A [\dot{g}_t w_t + g_t \dot{w}_t] \\ &= -r_t^T A [w_t w_t^T A^T r_t + g_t^2 P_{w_t^\perp} A^T r_t] \\ &= -(r_t^T A w_t)^2. \end{aligned}$$

From arguments similar to before, it follows that  $r_t^T A w_t \rightarrow 0$  as  $t \rightarrow \infty$ . Moreover, from a similar subsequence argument it also follows that  $w_t \rightarrow w$  such that  $r^T A w = 0$ . Since  $\|w\| = 1$  and  $A$  has full row rank, it follows that  $r = 0$ . Hence the flow converges to a zero of the loss. Moreover, since  $w \in R$ , it follows that this is the minimum norm solution.  $\square$

### C. Proof of Theorem 3.3

*Proof.* The proof proceeds similarly to that for WN flow: by calculating the derivatives of several quantities, and observing that there are some surprising invariants. First, let us write the ODE explicitly, using  $r_t = Ag_t u_t - b$ , as

$$\begin{aligned} \dot{g}_t &= -w_t^T A^T r_t \\ \dot{u}_t &= -g_t A^T r_t \\ w_t &= u_t / \|u_t\|. \end{aligned}$$

We notice the following two invariants:

$$\begin{aligned} \|u_t\| &= 1/2 \cdot g_t^2 \\ g_t \cdot \|w_t^\perp\|^2 &= C. \end{aligned}$$

To prove this, we will systematically calculate a few derivatives.

$$\dot{w}_t = d(u_t/\|u_t\|)/dt = \frac{\dot{u}_t\|u_t\| - u_t d\|u_t\|/dt}{\|u_t\|^2}.$$

$$d\|u_t\|/dt = u_t^T \dot{u}_t/\|u_t\| = w_t^T u_t = -g_t \nabla w_t^T A^T r_t.$$

$$d[1/2 \cdot g_t^2]/dt = g_t \dot{g}_t = -g_t \nabla w_t^T A^T r_t.$$

From the last two equations, it follows that  $d\|u_t\|/dt = d[1/2 \cdot g_t^2]/dt$ , and hence  $\|u_t\| - 1/2 \cdot g_t^2 = \|u_0\| - 1/2 \cdot g_0^2 = 0$ , where the last equality follows by the choice of the initialization. This proves one of the invariants. In particular, it also shows that if we reach  $u_t = 0$ , then we must also reach  $g_t = 0$  at that time (because the derivation above is correct up to that time). Now if  $g_t = 0$ , then we have that  $\dot{u}_t = 0$ , while  $w_t = 0$ , in which case  $\dot{g}_t = 0$ . We will show at the end of this proof that this case does not occur.

Continuing, we find

$$\dot{w}_t = (I - w_t w_t^T) \dot{u}_t/\|u_t\| = -Q_t g_t A^T r_t/\|u_t\|,$$

where we defined  $Q_t = I - w_t w_t^T$  to be the projection into the orthocomplement of  $w_t$ .

Now we can calculate the derivative of the loss as

$$\begin{aligned} d[1/2 \cdot \|r_t\|^2]/dt &= r_t^T \dot{r}_t = r_t^T A d(g_t w_t)/dt \\ &= r_t^T A [\dot{g}_t w_t + g_t \dot{w}_t]. \end{aligned}$$

So, by plugging in the gradients, we find

$$d[1/2 \cdot \|r_t\|^2]/dt = -r_t^T A M_t A^T r_t$$

where

$$M_t = w_t w_t^T + \frac{g_t^2}{\|u_t\|} (I - w_t w_t^T) = 2I - w_t w_t^T.$$

The last equality follows by the invariant  $\|u_t\| = 1/2 \cdot g_t^2$ . This last matrix has all eigenvalues greater than or equal than unity. Hence,

$$d[1/2 \cdot \|r_t\|^2]/dt \leq -\|A^T r_t\|^2 \leq -\lambda_{\min}(AA^T) \|r_t\|^2.$$

This implies that the loss converges geometrically to the global minimum.

Finally, to characterize which solution we converge to, we study the dynamics of  $w_t^\perp$ . The intuition for doing so is that we hope that our algorithm will decrease this component, and get closer to the min norm solution, and so we hope to be able to see it from its dynamics. Explicitly, we have  $w_t^\perp = P w_t$ , where  $P$  is the linear projection operator in the the orthocomplement of the row space of  $A$ . Then

$$d[1/2 \cdot \|w_t^\perp\|^2]/dt = w_t^{\perp,T} \dot{w}_t^\perp.$$

Now

$$\dot{w}_t^\perp = P \dot{w}_t = -P Q_t g_t A^T r_t/\|u_t\| = P w_t w_t^T A^T r_t/(2g_t).$$

Thus

$$\begin{aligned} d[1/2 \cdot \|w_t^\perp\|^2]/dt &= w_t^\perp P w_t w_t^T A^T r_t/(2g_t) \\ &= -\|w_t^\perp\|^2 \cdot \dot{g}_t/(2g_t). \end{aligned}$$

In this equation we have used the form of the derivative  $\dot{g}_t$ . This shows that the we have the equality

$$\frac{d[\|w_t^\perp\|^2]/dt}{\|w_t^\perp\|^2} + \frac{\dot{g}_t}{g_t} = 0$$

Hence by the product rule we conclude that  $g_t \cdot \|w_t^\perp\|^2$  is invariant.

Now we want to argue that we never reach  $g_t = 0$ . As we have seen, this is equivalent to  $\|u_t\| = 0$ . Thus, the argument above holds up until the point  $t^*$  where these happen. Thus, the above invariance also holds, and so we get a contradiction, because  $g_t$  is lower bounded, as  $\|w_t^\perp\| \leq 1$ .

This finishes the proof.  $\square$

## D. Proof of Theorem 4.1

We restate Theorem 4.1 here.

**Theorem D.1** (Updating  $g$  in Phase I). *Suppose we initialize with  $g_0 < g^*$ . Let  $\delta_0 = (g^*)^2 - (g_0)^2 > 0$  and  $\delta < \frac{\varepsilon}{2g^* + \varepsilon}$ . Suppose the number of iterations  $T_1$  and  $T_2$  is of the order:*

$$T_1 = \left(1 + \frac{2(g^*)^2 + \delta_0}{\delta_0}\right) \log \left(\frac{1 - \|Aw_0\|}{\delta}\right) = \mathcal{O} \left(\frac{(g^*)^2}{\delta_0} \log \left(\frac{1}{\varepsilon}\right)\right),$$

$$T_2 = \frac{1}{\gamma^{(2)}} \log \left(\frac{\|Aw_0\|}{g^* \varepsilon}\right) = \mathcal{O} \left(\frac{1}{\gamma^{(2)}} \log \left(\frac{1}{\varepsilon}\right)\right).$$

Fix  $g_1 = g_0$  at the first step. For iterations  $t = 1, \dots, T_1 - 1$ , set the stepsize for  $g$  to

$$\gamma^{(1)} < \min \left\{ \frac{g_0^2}{2T_1((g^*)^2 - \|Ag_0w_0\|^2)} \log \left(\frac{1}{2} \left(\frac{(g^*)^2}{g_0^2} + 1\right)\right), \frac{1}{2(1 + \|Aw_0\|^2)} \right\}$$

and to any  $\gamma^{(2)} \leq \frac{1}{4}$  for  $t = T_1, T_1 + 1, \dots, T_1 + T_2 - 1$ . Set  $\eta_t = 1/g_t^2$ . Then we reach  $\|w_T^\perp\|^2 \leq \varepsilon$  and  $\|Ag_T w_T - b\| \leq \varepsilon$  after  $T = T_1 + T_2$  iterations.

*Proof.* By Lemma E.3,

$$\|A(g_{t+1}w_{t+1} - g^*w^*)\|^2 = \|r_t\|^2 \leq (g_{t+1} - g_t\|v_t\|)^2$$

which means we only need to analyze the dynamics of  $g_{t+1} - g_t\|v_t\|$ . Lemma E.1 (equation equation 31) implies the positiveness of this term  $g_t\|v_t\| - g_{t+1} > 0$ , and so we just need to analyze the term:

$$\|A(g_{t+1}w_{t+1} - g^*w^*)\| = g_t\|v_t\| - g_{t+1}$$

By the update of  $g_t$  and by Lemma E.4

$$g_t\|v_t\| - g_{t+1} = (1 - \gamma^{(1)})(g_{t-1}\|v_{t-1}\| - g_t) \tag{26}$$

$$- (g_{t-1}\|v_{t-1}\| - g_t\|v_t\|) \left(1 - \frac{\gamma^{(1)}}{g_t} \frac{g_{t-1}\|v_{t-1}\|}{(g_t + g_{t-1}\|v_{t-1}\|)} (g_t\|v_t\| + g_{t-1}\|v_{t-1}\|)\right). \tag{27}$$

Observe that Lemma E.5 with equation 32 implies that

$$g_{t-1}\|v_{t-1}\| - g_t\|v_t\| > 0.$$

Meanwhile, with Lemma E.2 and Lemma E.5, we have

$$\frac{g_t(g_t + g_{t-1}\|v_{t-1}\|)}{g_{t-1}\|v_{t-1}\|(g_t\|v_t\| + g_{t-1}\|v_{t-1}\|)} \geq \frac{g_t^2}{g_{t-1}\|v_{t-1}\|(g_t\|v_t\| + g_{t-1}\|v_{t-1}\|)} \geq \frac{g_0^2}{2g_0^2\|v_0\|^2} = \frac{1}{2\|v_0\|^2} \geq \frac{1}{2(1 + \|Aw_0\|^2)}$$

By our choice of  $\gamma^{(1)}$ ,

$$\gamma^{(1)} \leq \frac{1}{2\|v_0\|^2} \leq \frac{g_t(g_t + g_{t-1}\|v_{t-1}\|)}{g_{t-1}\|v_{t-1}\|(g_t\|v_t\| + g_{t-1}\|v_{t-1}\|)}.$$

We have from equation 27 that

$$\begin{aligned}
g_t \|v_t\| - g_{t+1} &\leq (1 - \gamma^{(1)})^t (g_0 \|v_0\| - g_1) \\
&= (1 - \gamma^{(1)})^t (g_0 \|v_0\| - g_0) \\
&= (1 - \gamma^{(1)})^t \left( \frac{g^*}{\|Aw_0\|} - g_0 \right).
\end{aligned} \tag{28}$$

where the equality is due to  $g_1 = g_0$  at the first step.

On the other hand, we need an upper bound of  $g_t$  to see how the norm of  $1 - \|Aw_t\|^2$  evolves. To see this, notice that we use Lemma E.4:

$$g_{t+1} \leq g_t + \frac{\gamma g_t}{2} (\|v_t\|^2 - 1)$$

Thus,  $g_t$  grows with the rate  $\gamma^{(1)}(\|v_{t-1}\|^2 - 1)$ . We set  $\gamma^{(1)}$  very small such that after  $T_1$  there is a gap between  $g^*$  and  $g_{T_1}$ . We let the gap satisfies  $(g^*)^2 - g_{T_1}^2 \geq \frac{1}{2}\delta_0$ :<sup>6</sup>

$$g_{T_1+1}^2 \leq \prod_{t=1}^{T_1+1} \left( 1 + \frac{1}{2} \gamma^{(1)} (\|v_{t-1}\|^2 - 1) \right)^2 g_1^2 \leq \exp\left(\gamma^{(1)}(\|v_0\|^2 - 1)T_1\right) g_0^2 \leq (g^*)^2 - \frac{1}{2}\delta_0$$

where at the second step due to  $g_1 = g_0$  and the last step we use our choice of  $\gamma^{(1)}$  for fixed  $T_1$ ,  $g_0$ , and  $\delta_0$ . Observe that we have

$$(g^*)^2 - \|Ag_{T_1} w_{T_1}\|^2 \geq (g^*)^2 - g_{T_1}^2 = \frac{1}{2}\delta_0$$

By Lemma E.6, we have

$$(1 - \|Aw_{T_1}\|^2) \leq \exp\left(-\sum_{i=1}^{T_1} \frac{(g^*)^2 - \|Ag_i w_i\|^2}{(g^*)^2 + (g^*)^2 - \|Ag_i w_i\|^2}\right) (1 - \|Aw_0\|^2) \tag{29}$$

$$\leq \exp\left(-\frac{\delta_0 T_1}{2(g^*)^2 + \delta_0}\right) (1 - \|Aw_0\|^2) \tag{30}$$

we have  $\|w_{T_1}^\perp\|^2 = 1 - \|Aw_{T_1}\|^2 \leq \delta$  when

$$T_1 = \left(1 + \frac{2(g^*)^2 + \delta_0}{\delta_0}\right) \log\left(\frac{1 - \|Aw_0\|}{\delta}\right).$$

After  $T = T_1 + T_2$ , we have

$$\begin{aligned}
g_T \|v_T\| - g_T &\leq \exp(-\gamma^{(2)}(T_1 + T_2)) \left( \frac{g^*}{\|Aw_0\|} - g_0 \right) \\
&\leq \exp(-\gamma^{(2)}(T_1)) \frac{g^*}{\|Aw_0\|}.
\end{aligned}$$

So we have  $g_T \|v_T\| - g_T \leq \varepsilon$ .

□

## E. Technical Lemmas for Theorem 4.1 and 4.2

In the following section, we assume  $AA^\top = I_{m \times m}$  and use  $r_t = A(g_t w_t - g^* w^*)$  to denote the negative residual.

<sup>6</sup>Note that one could pick any gap  $c = (g^*)^2 - g_{T_1}^2$ ,  $c \leq 0$ , we use  $\frac{1}{2}\delta_0$  is for the convenience of the proof.

**Lemma E.1.** With the step-size  $\eta = \frac{1}{g_t^2}$ , we have the following equalities:

$$g_t^2 \|v_t\|^2 = g_t^2 + ((g^*)^2 - \|Ag_t w_t\|^2) \quad (31)$$

$$\|g_t\| \|v_t\| = \frac{g^*}{\|Aw_{t+1}\|} \quad (32)$$

$$\|Aw_{t+1}\|^2 = \frac{(g^*)^2}{(g^*)^2 + g_t^2(1 - \|Aw_t\|^2)} \quad (33)$$

$$1 - \|Aw_{t+1}\|^2 = \frac{1}{\|v_t\|^2} (1 - \|Aw_t\|^2) \quad (34)$$

$$g_{t+1}^2 - \|Ag_{t+1} w_{t+1}\|^2 = \frac{\|Ag_{t+1} w_{t+1}\|^2}{(g^*)^2} (g_t^2 - \|Ag_t w_t\|^2). \quad (35)$$

*Proof.* With the update of  $w_t$ :

$$w_{t+1} = w_t - \eta g_t A^\top r_t, \quad v_{t+1} = \frac{v_t}{\|v_t\|},$$

we can get that:

$$\begin{aligned} \|v_t\|^2 &= \|w_t\|^2 - 2\eta \langle Ag_t w_t, r_t \rangle + \eta^2 g_t^2 \|r_t\|^2 \\ &= 1 + \eta (\|Ag^* w^*\|^2 - \|Ag_t w_t\|^2 - \|r_t\|^2) + \eta^2 g_t^2 \|r_t\|^2 \end{aligned}$$

Moreover:

$$\begin{aligned} \|Aw_{t+1}\|^2 &= \frac{1}{\|v_t\|^2} \|Aw_t - \eta g_t r_t\|^2 \\ \Leftrightarrow \|v_t\|^2 \|Aw_{t+1}\|^2 &= \|Aw_t\|^2 - 2\eta \langle Ag_t w_t, r_t \rangle + \eta^2 g_t^2 \|r_t\|^2 \\ &= \|Aw_t\|^2 - 2\eta \langle Ag_t w_t, r_t \rangle + \eta^2 g_t^2 \|r_t\|^2 \\ &= \|Aw_t\|^2 + \eta (\|Ag^* w^*\|^2 - \|Ag_t w_t\|^2 - \|r_t\|^2) + \eta^2 g_t^2 \|r_t\|^2. \end{aligned}$$

Letting  $\eta = \frac{1}{g_t^2}$ , we have:

$$\begin{aligned} g_t^2 \|v_t\|^2 &= g_t^2 + ((g^*)^2 - \|Ag_t w_t\|^2) \\ \|v_t\|^2 \|Aw_{t+1}\|^2 &= \frac{(g^*)^2}{g_t^2}. \end{aligned}$$

Combining equation 31 and equation 32, we can get equation 33, and with equation 33, we can obtain equation 35 and equation 34 after some algebra.  $\square$

**Lemma E.2.** If  $\eta = \frac{1}{g_t^2}$ , we always have that

$$g_{t+1} > g_t, \quad \forall t$$

*Proof.* Notice that  $g_{t+1} = g_t - \gamma \langle Aw_t, r_t \rangle$ , so we only need to prove that  $\langle Aw_t, r_t \rangle < 0$ . We have the following property:

$$Aw_{t+1} = \frac{Aw_t - \frac{1}{g_t} r_t}{\|v_t\|} = \frac{Ag^* w^*}{g_t \|v_t\|},$$

which can lead to:

$$\langle Aw_t, r_t \rangle = g_t \|Aw_t\|^2 - g^* \langle Aw_t, Aw^* \rangle = g_t \frac{(g^*)^2}{g_t^2 \|v_t\|^2} - \frac{(g^*)^2}{g_t \|v_t\|} = \frac{(g^*)^2}{g_t \|v_t\|^2} (1 - \|v_t\|) < 0,$$

that finishes the proof.  $\square$

**Lemma E.3.** Assuming  $\eta = \frac{1}{g_t^2}$ , we have

$$\|r_{t+1}\|^2 = (g_{t+1} - g_t \|v_t\|)^2 + \left(\frac{g_{t+1}^2}{\|v_t\|^2} - g_t^2\right)(\|Aw_t\|^2 - 1) \leq (g_{t+1} - g_t \|v_t\|)^2. \quad (36)$$

*Proof.* Let  $\alpha_t = \frac{g_{t+1}}{g_t \|v_t\|} - 1$ . We start by considering the loss as a function of  $x_t := g_t w_t$ . Notice that, for any  $L$ -smooth loss  $f$ , we have

$$f(x_{t+1}) - f(x^*) \leq f(x_t) - f(x^*) + \langle \nabla_x f(x_t), x_{t+1} - x_t \rangle + \frac{L}{2} \|x_{t+1} - x_t\|^2$$

where  $L$  is the smoothness constant. By using the gradient update for  $w_{t+1}$ , we have:

$$\begin{aligned} x_{t+1} - x_t &= \left(\frac{g_{t+1}}{g_t \|v_t\|} - 1\right) g_t w_t - \frac{\eta g_{t+1} g_t}{\|v_t\|} A^\top r_t \\ &= \alpha_t g_t w_t - \frac{g_{t+1}}{g_t \|v_t\|} A^\top r_t, \end{aligned}$$

which leads to

$$\|x_{t+1} - x_t\|^2 = \alpha_t^2 g_t^2 \|w_t\|^2 + \frac{g_{t+1}^2}{g_t^2 \|v_t\|^2} \|r_t\|^2 - 2\alpha_t \frac{g_{t+1}}{g_t \|v_t\|} \langle Ag_t w_t, r_t \rangle.$$

If we use  $f(x_t) = \frac{1}{2} \|r_t\|^2$ , then  $\nabla_x f(x_t) = A^\top r_t$ . The smoothness constant is  $L = 1$  for orthogonal  $A$ , so we can get that:

$$\begin{aligned} \langle \nabla_x f(x_t), x_{t+1} - x_t \rangle &= \langle r_t, \alpha_t Ag_t w_t - \frac{g_{t+1}}{g_t \|v_t\|} r_t \rangle \\ &= \alpha_t \langle r_t, Ag_t w_t \rangle - \frac{g_{t+1}}{g_t \|v_t\|} \|r_t\|^2. \end{aligned}$$

Summing up we get:

$$\begin{aligned} f(x_{t+1}) - f(x_t) &\leq \frac{1}{2} \alpha_t^2 g_t^2 \|w_t\|^2 + \frac{g_{t+1}}{2g_t \|v_t\|} \left(\frac{g_{t+1}}{g_t \|v_t\|} - 2\right) \|r_t\|^2 \\ &\quad - \alpha_t \left(\frac{g_{t+1}}{g_t \|v_t\|} - 1\right) \langle Ag_t w_t, r_t \rangle. \end{aligned}$$

Denoting  $b_t = \langle Ag_t w_t, r_t \rangle$ , we can write

$$\begin{aligned} f(x_{t+1}) - f(x_t) &\leq \frac{g_{t+1}}{2g_t \|v_t\|} \left(\frac{g_{t+1}}{g_t \|v_t\|} - 2\right) \|r_t\|^2 + \frac{1}{2} \alpha_t^2 g_t^2 - \alpha_t^2 b_t \\ &= \frac{1}{2} (\alpha_t + 1)(\alpha_t - 1) \|r_t\|^2 + \frac{1}{2} \alpha_t^2 (g_t^2 - 2b_t) \\ &= (\alpha_t + 1)(\alpha_t - 1) f(x_t) + \frac{1}{2} \alpha_t^2 (g_t^2 - 2b_t) \quad \text{Note } f(x_t) = \frac{1}{2} \|r_t\|^2 \\ \Rightarrow f(x_{t+1}) &\leq \alpha_t^2 f(x_t) + \frac{1}{2} \alpha_t^2 (g_t^2 - 2b_t) \\ \Leftrightarrow \|r_{t+1}\|^2 &\leq \alpha_t^2 \|r_t\|^2 + \alpha_t^2 (g_t^2 - 2b_t). \end{aligned}$$

Notice that  $-2b_t = (g^*)^2 - \|Ag_t w_t\|^2 - \|r_t\|^2$ , thus

$$\begin{aligned} \|r_{t+1}\|^2 &\leq \alpha_t^2 (g_t^2 + (g^*)^2 - \|Ag_t w_t\|^2) \\ &= \alpha_t^2 g_t^2 \|v_t\|^2 \quad \text{Recall } \|v_t\|^2 = 1 + \frac{1}{g_t^2} ((g^*)^2 - \|Ag_t w_t\|^2) \\ &= (g_{t+1} - g_t \|v_t\|)^2. \end{aligned}$$

Moreover, we have that

$$\|r_{t+1}\|^2 = \alpha_t^2 (g^*)^2 = (g_{t+1} - g_t \|v_t\|)^2 + \alpha_t^2 g_t^2 (\|Aw_t\|^2 - 1) \quad (37)$$

To see this, we only need to show that

$$\frac{1}{2} \|r_{t+1}\|^2 = \frac{1}{2} \|r_t\|^2 + \langle \nabla_x f(x_t), x_{t+1} - x_t \rangle + \frac{1}{2} \|Ax_{t+1} - Ax_t\|^2 \quad (38)$$

which is obvious.  $\square$

**Lemma E.4.** For  $\eta = \frac{1}{g_t^2}$ , we have the following equality (where  $\gamma = \gamma_t$ ):

$$g_{t+1} \leq g_t + \frac{\gamma g_t}{2} (\|v_t\|^2 - 1)$$

$$g_t \|v_t\| - g_{t+1} = (1 - \gamma)(g_{t-1} \|v_{t-1}\| - g_t) - (g_{t-1} \|v_{t-1}\| - g_t \|v_t\|) \left( 1 - \frac{\gamma}{g_t} \frac{g_{t-1} \|v_{t-1}\|}{(g_t + g_{t-1} \|v_{t-1}\|)} (g_t \|v_t\| + g_{t-1} \|v_{t-1}\|) \right)$$

*Proof.* The update of  $g_{t+1}$  is

$$\begin{aligned} g_{t+1} &= g_t - \gamma \langle Aw_t, r_t \rangle \\ &= g_t + \frac{\gamma}{2g_t} ((g^*)^2 - \|Ag_t w_t\|^2 - \|r_t\|^2) \\ &= g_t + \frac{\gamma g_t}{2} (\|v_t\|^2 - 1) - \frac{\gamma}{2g_t} \|r_t\|^2. \end{aligned}$$

where the second equality due to  $\langle Ag_t w_t, r_t \rangle = \|Ag^* w^*\|^2 - \|Ag_t w_t\|^2 - \|r_t\|^2$  and the last equality due to update of  $\|v_t\|$  (see equality 31). This finishes the proof for the first inequality.

Denoting  $C_t = \alpha_{t-1}^2 g_{t-1}^2 (\|Aw_{t-1}\|^2 - 1)$ , we get

$$\begin{aligned} g_{t+1} &= g_t + \frac{\gamma}{2g_t} g_t^2 (\|v_t\|^2 - 1) - \frac{\gamma}{2g_t} \|r_t\|^2 \\ &= g_t + \frac{\gamma g_t}{2} \|v_t\|^2 - \frac{\gamma g_t}{2} - \frac{\gamma}{2g_t} ((g_{t-1} \|v_{t-1}\| - g_t)^2 + C_t) \\ &= g_t + \frac{\gamma g_t}{2} \|v_t\|^2 - \frac{\gamma g_t}{2} - \frac{\gamma}{2g_t} ((g_{t-1}^2 \|v_{t-1}\|^2 + g_t^2 - 2g_t g_{t-1} \|v_{t-1}\|) + C_t) \\ &= g_t + \frac{\gamma g_t}{2} \|v_t\|^2 - \frac{\gamma}{2g_t} g_{t-1}^2 \|v_{t-1}\|^2 + \gamma (g_{t-1} \|v_{t-1}\| - g_t) - \frac{\gamma}{2g_t} C_t \\ &= g_t + \frac{\gamma}{2g_t} (g_t^2 \|v_t\|^2 - g_{t-1}^2 \|v_{t-1}\|^2) + \gamma (g_{t-1} \|v_{t-1}\| - g_t) - \frac{\gamma}{2g_t} C_t \\ \Rightarrow g_t \|v_t\| - g_{t+1} &= g_t \|v_t\| - g_t - \frac{\gamma}{2g_t} (g_t^2 \|v_t\|^2 - g_{t-1}^2 \|v_{t-1}\|^2) - \gamma (g_{t-1} \|v_{t-1}\| - g_t) + \frac{\gamma}{2g_t} C_t \\ &= (1 - \gamma)(g_{t-1} \|v_{t-1}\| - g_t) - g_{t-1} \|v_{t-1}\| + g_t \|v_t\| \\ &\quad - \underbrace{\frac{\gamma}{2g_t} (g_t^2 \|v_t\|^2 - g_{t-1}^2 \|v_{t-1}\|^2) + \frac{\gamma}{2g_t} \alpha_{t-1}^2 g_{t-1}^2 (\|Aw_{t-1}\|^2 - 1)}_{Term1}. \end{aligned}$$

We prove the lemma with following simplification for  $Term1$ :

$$\begin{aligned}
Term1 &= -\frac{\gamma}{2g_t} (g_t^2 \|v_t\|^2 - g_{t-1}^2 \|v_{t-1}\|^2) + \frac{\gamma}{2g_t} \alpha_{t-1}^2 g_{t-1}^2 (\|Aw_{t-1}\|^2 - 1) \\
&= -\frac{\gamma}{2g_t} \left( \frac{g_t^2}{\|v_{t-1}\|^2} - g_{t-1}^2 \right) (1 - \|Aw_{t-1}\|^2) + \frac{\gamma}{2g_t} \alpha_{t-1}^2 g_{t-1}^2 (\|Aw_{t-1}\|^2 - 1) \\
&= -\frac{\gamma}{2g_t} (1 - \|Aw_{t-1}\|^2) \left( \frac{g_t^2}{\|v_{t-1}\|^2} - g_{t-1}^2 - \left( \frac{g_t}{\|v_{t-1}\|} - g_{t-1} \right)^2 \right) \\
&= -\frac{\gamma}{2g_t} (1 - \|Aw_{t-1}\|^2) \left( \frac{2g_t g_{t-1}}{\|v_{t-1}\|} - 2g_{t-1}^2 \right) \\
&= -\frac{\gamma g_{t-1}}{g_t} (1 - \|Aw_{t-1}\|^2) \left( \frac{g_t}{\|v_{t-1}\|} - g_{t-1} \right) \\
&= -\frac{\gamma g_{t-1} \|v_{t-1}\|}{g_t} \frac{g_t^2 \|v_t\|^2 - g_{t-1}^2 \|v_{t-1}\|^2}{g_t + g_{t-1} \|v_{t-1}\|}
\end{aligned}$$

where at the last step we use Lemma E.5 to have:

$$\begin{aligned}
(1 - \|Aw_{t-1}\|^2) \left( \frac{g_t}{\|v_{t-1}\|} - g_{t-1} \right) &= \frac{1}{\frac{g_t}{\|v_{t-1}\|} + g_{t-1}} (1 - \|Aw_{t-1}\|^2) \left( \frac{g_t^2}{\|v_{t-1}\|^2} - g_{t-1}^2 \right) \\
&= \frac{g_t^2 \|v_t\|^2 - g_{t-1}^2 \|v_{t-1}\|^2}{\frac{g_t}{\|v_{t-1}\|} + g_{t-1}} \\
&= \|v_{t-1}\| \frac{g_t^2 \|v_t\|^2 - g_{t-1}^2 \|v_{t-1}\|^2}{g_t + g_{t-1} \|v_{t-1}\|}
\end{aligned}$$

□

**Lemma E.5.** We have the following identity for the recursion on  $g_t^2 \|v_t\|^2$ :

$$g_t^2 \|v_t\|^2 - g_{t-1}^2 \|v_{t-1}\|^2 = \left( \frac{g_t^2}{\|v_{t-1}\|^2} - g_{t-1}^2 \right) (1 - \|Aw_{t-1}\|^2) = (g_t^2 - g_{t-1}^2 \|v_{t-1}\|^2) (1 - \|Aw_t\|^2) \leq 0.$$

*Proof.* By Lemma E.1, we use the equation 31 to get

$$\begin{aligned}
g_t^2 \|v_t\|^2 - g_{t-1}^2 \|v_{t-1}\|^2 &= g_t^2 (1 - \|Aw_t\|^2) - g_{t-1}^2 (1 - \|Aw_{t-1}\|^2) \\
&= \left( \frac{g_t^2}{\|v_{t-1}\|^2} - g_{t-1}^2 \right) (1 - \|Aw_{t-1}\|^2) \\
&= (g_t^2 - g_{t-1}^2 \|v_{t-1}\|^2) (1 - \|Aw_t\|^2).
\end{aligned}$$

□

Notice that with equation 32, we have that  $g_t \|v_t\| < g_{t-1} \|v_{t-1}\|$

**Lemma E.6.** We have the following bound on the closeness of  $Aw_t$  to unit norm:

$$(1 - \|Aw_t\|^2) \leq \exp\left(-\sum_{i=1}^t \frac{(g^*)^2 - \|Ag_i w_i\|^2}{(g^*)^2 + (g^*)^2 - \|Ag_i w_i\|^2}\right) (1 - \|Aw_0\|^2). \quad (39)$$

*Proof.* If we keep  $g_t \leq g^*$ , by equation 33 we always have that

$$\begin{aligned}
1 - \|Aw_{t+1}\|^2 &= \frac{g_t^2 (1 - \|Aw_t\|^2)}{(g^*)^2 + g_t^2 (1 - \|Aw_t\|^2)} \\
&\leq \frac{(g^*)^2}{(g^*)^2 + (g^*)^2 - \|Ag_t w_t\|^2} (1 - \|Aw_t\|^2) \\
&\leq \exp\left(-\frac{(g^*)^2 - \|Ag_t w_t\|^2}{(g^*)^2 + (g^*)^2 - \|Ag_t w_t\|^2}\right) (1 - \|Aw_0\|^2).
\end{aligned}$$



The first inequality holds due to

$$\frac{g_t^2}{(g^*)^2 + g_t^2(1 - \|Aw_t\|^2)} \leq \frac{g_t^2 + ((g^*)^2 - g_t^2)}{(g^*)^2 + g_t^2(1 - \|Aw_t\|^2) + ((g^*)^2 - g_t^2)}$$

Thus,

$$(1 - \|Aw_t\|^2) \leq \exp\left(-\sum_{i=1}^t \frac{(g^*)^2 - \|Ag_i w_i\|^2}{(g^*)^2 + (g^*)^2 - \|Ag_i w_i\|^2}\right)(1 - \|Aw_0\|^2).$$

□

**Lemma E.7.** *We have following property in Phase II for Theorem 4.2*

- *Property (i):*  $\|w_{t+1}^\perp\| \leq \|w_t^\perp\| \leq \varepsilon$ .
- *Property (ii):* letting  $\gamma' = \gamma(1 - \varepsilon^2)$ , we have

$$(1 - \gamma')g_t + \gamma'g^* \leq g_{t+1} \leq g^*.$$

*Proof.* We will argue by induction. We first show that the above two properties hold when  $t = T_1$ . Since  $g_{T_1} = g_0 < g^*$ , by (18), we have  $\|w_{T_1+1}^\perp\| \leq g_{T_1} \|w_{T_1}^\perp\|/g^* < \|w_{T_1}^\perp\| \leq \varepsilon$ . By (20), we have

$$\begin{aligned} g_{T_1+1} &\stackrel{(a)}{\leq} g_{T_1} - \gamma g_{T_1}(1 - \varepsilon^2) + \gamma g^* \\ &= g_{T_1} - \gamma g_{T_1}(1 - \varepsilon^2) + \gamma(1 - \varepsilon^2)g^* + \gamma\varepsilon^2 g^* \\ &\stackrel{(b)}{=} g_0 - \gamma'g_0 + \gamma'g^* + \gamma'\delta \\ &= g^* - (1 - \gamma')(g^* - g_0) + \gamma'\delta, \end{aligned} \tag{40}$$

and

$$\begin{aligned} g_{T_1+1} &\stackrel{(c)}{\geq} g_{T_1} - \gamma g_{T_1} \|w_{T_1}^\perp\|^2 + \gamma g^* \|w_{T_1}^\perp\|^2 \\ &= g_{T_1} + \gamma(g^* - g_{T_1}) \|w_{T_1}^\perp\|^2 \\ &\stackrel{(d)}{\geq} g_{T_1} + \gamma(g^* - g_{T_1})(1 - \varepsilon^2) \\ &= (1 - \gamma')g_{T_1} + \gamma'g_{T_1}, \end{aligned} \tag{41}$$

where inequalities (a), (c), and (d) follow from the fact that  $1 - \varepsilon^2 \leq \|w_{T_1}^\perp\|^2 \leq 1$ , and (b) follows from our definition  $\gamma' = \gamma(1 - \varepsilon^2)$ ,  $\delta = \varepsilon^2 g^*/(1 - \varepsilon^2)$ , and the fact that  $g_{T_1} = g_0 < g^*$ . By the upper bound of  $\gamma$  given in (12), we can verify that  $(1 - \gamma')(g^* - g_0) > \gamma'\delta$ , and hence, (40) implies that  $g_{T_1+1} < g^*$ .

Now suppose that Property (i) and (ii) hold for  $t = T_1, \dots, k-1$ , where  $T_1 \leq k-1 < T_1 + T_2 - 1$ . We need to prove that they also hold for the  $k$ -th iteration. By assumption,  $g_k \leq g^*$ , so using the same argument as (17) and (18), we have  $\|v_k\|^2 \geq 1$  and  $\|w_{k+1}^\perp\| = \|w_k^\perp\|/\|v_k\| \leq \|w_k^\perp\| \leq \varepsilon$ , where the last step follows from Property (i) at the  $(k-1)$ -th iteration. Therefore, Property (i) holds for the  $k$ -th iteration.

To prove Property (ii), first note that by assumption,  $1 - \varepsilon^2 \leq \|w_k^\perp\|^2 \leq 1$ . We can use the same argument as (41) to show that  $g_{k+1} \geq (1 - \gamma')g_k + \gamma'g^*$ . We can also use a similar argument as (40) to get

$$g_{k+1} \leq g^* - (1 - \gamma')(g^* - g_k) + \gamma'\delta, \tag{42}$$

where  $\gamma' = \gamma(1 - \varepsilon^2)$  and  $\delta = \varepsilon^2 g^*/(1 - \varepsilon^2)$ . The above equation can be rewritten as

$$\begin{aligned} g^* - g_{k+1} + \delta &\geq (1 - \gamma')(g^* - g_k + \delta) \\ &\geq (1 - \gamma')^{k+1-T_1}(g^* - g_{T_1} + \delta) \\ &\stackrel{(a)}{\geq} (1 - \gamma')^{T_2}(g^* - g_0 + \delta) \\ &\stackrel{(b)}{=} \delta, \end{aligned} \tag{43}$$

where (a) follows from the fact that  $k \leq T_1 + T_2 - 1$ , and (b) can be verified for our choice of  $T_2$ . Eq. (43) implies that  $g_{k+1} \leq g^*$ . □

## F. General A matrix

**Lemma F.1** (For all  $w^*$ ). *Let  $\sigma_i$  be the singular values of  $A$  in decreasing order, let  $r$  be the rank of  $A$ , so that  $\sigma_r > 0$ . We fix  $g := g_0$  satisfying*

$$g_0 \leq \frac{g^* \sigma_r}{2 + \delta - \sigma_r}$$

*and update only  $w$  using rPGD. Then we have the orthogonal component  $w^\perp$  decreases geometrically such that  $\|w_{T_1}^\perp\| \leq \epsilon$  after iteration*

$$T_1 = \frac{1}{\log(1 + \delta)} \log \left( \frac{\|w_0^\perp\|}{\epsilon} \right)$$

*Proof.* Consider the singular value decomposition of  $A^\top A = U \Sigma U^\top$  with

$$\Sigma = \begin{bmatrix} \sigma_1 & & & & \\ & \ddots & & & \\ & & \sigma_m & & \\ & & & \mathbf{0}_{d-m} & \end{bmatrix} \quad \text{with } 1 = \sigma_1 \geq \sigma_2 \geq \dots \geq \sigma_m > 0. \quad (44)$$

Moreover  $U$  is a  $d \times d$  orthogonal matrix. We now use superscripts  $t$  to illustrate the  $t$ th iteration  $w_t$  since we use subscript for the eigenvalues index. Let  $\eta = \frac{1}{g_t^2 \sigma_1} = \frac{1}{g_t^2}$ . The update of  $v_t$  can be written as

$$v_t = w_t - \eta g_0 A^\top A (g_0 w_t - g^* w^*) = (I - A^\top A) w_t + \frac{g^*}{g_0} A^\top A w^* = U (I - \Sigma) U^\top w_t + \frac{g^*}{g_0} U \Sigma U^\top w^*$$

$$\begin{aligned} \|v_t\| &= \left\| \frac{g^*}{g_0} \Sigma U^\top w^* + (I - \Sigma) U^\top w_t \right\| \\ &= \left\| \frac{g^*}{g_0} \begin{bmatrix} \sigma_1 & & & \\ & \ddots & & \\ & & \sigma_m & \\ & & & \mathbf{0}_{d-m} \end{bmatrix} U^\top w^* + \begin{bmatrix} 0 & & & \\ & \ddots & & \\ & & 0 & \\ & & & \mathbf{1}_{d-m} \end{bmatrix} U^\top w_t + \begin{bmatrix} 1 - \sigma_1 & & & \\ & \ddots & & \\ & & 1 - \sigma_m & \\ & & & \mathbf{0}_{d-m} \end{bmatrix} U^\top w_t \right\| \\ &\geq \sqrt{\left( \frac{g^*}{g_0} \right)^2 \sum_{i=1}^m \sigma_i^2 [U^\top w^*]_i^2 + \sum_{i=m+1}^d [U^\top w_t]_i^2} - \sqrt{\sum_{i=1}^m (1 - \sigma_i)^2 [U^\top w_t]_i^2} \\ &\geq \frac{g^*}{g_0} \sigma_m - (1 - \sigma_m) \\ &\geq \left( \frac{g^*}{g_0} + 1 \right) \sigma_m - 1 \\ &\geq 1 + \delta \end{aligned} \quad (45)$$

since we have

$$\sigma_m \geq \frac{2 + \delta}{\left( \frac{g^*}{g_0} + 1 \right)} \Leftrightarrow g_0 \leq \frac{g^* \sigma_m}{2 + \delta - \sigma_m} \text{ and } \sigma_m \leq 2$$

Note that the singular values are sorted so that  $\sigma_m \leq \sigma_1 = 1$ , so the second inequality clearly holds. The above inequality implies that as long as we have  $g_0$  small, we can always guarantee  $\|v\| \geq 1 + \delta$ . Using the equality

$$\|w_{t+1}^\perp\| = \frac{\|w_t^\perp\|}{\|v_{t+1}\|} \leq \frac{1}{1 + \delta} \|w_t^\perp\|$$

we see that the orthogonal component  $w^\perp$  decreases geometrically.  $\square$

**Lemma F.2** (random vector  $w^*$  uniformly distributed on the sphere). *Suppose further that  $w^*$  is randomly drawn on the sphere, i.e.  $w^* = \frac{z}{\|z\|}$  where  $z \sim \mathcal{N}(0, I_d)$ . If the input data matrix  $A$  satisfies :*

- the maximum eigenvalue of  $\lambda_{\max}(AA^\top) = 1$
- the rank of  $AA^\top$  is  $m$ .
- the spectral of  $A \in \mathbb{R}^{m \times d}$  satisfies  $\frac{1}{m} \left( \|AA^\top\|_F^2 - 2\sqrt{m \log(m)} \right) \geq \sigma_m^2$  where the  $\sigma_m$  is the minimum eigenvalue of  $AA^\top$ .

Then we can fix  $g := g_0$  satisfying

$$g_0 \leq \frac{g^*}{(2 + \delta - \sigma_m)} \sqrt{\frac{\|AA^\top\|_F^2 - 2\sqrt{m \log(m)}}{m}}$$

and update only  $w$  using rPGD. Then with probability  $1 - \mathcal{O}(\frac{1}{m})$ , we have the orthogonal component  $w^\perp$  decreases geometrically such that  $\|w_{T_1}^\perp\| \leq \epsilon$  after iteration

$$T_1 = \frac{1}{\log(1 + \delta)} \log \left( \frac{\|w_0^\perp\|}{\epsilon} \right)$$

*Proof.* Since  $w^*$  is uniform on the  $d$ -dimensional sphere,  $u^* := U^\top w^*$  (let  $[U^\top w^*]_i = u_i^*$ ) is also uniform on the  $d$ -dimensional sphere. Moreover, we can represent the random vector  $u^*$  as a standard Normal random vector divided by its norm, i.e.

$$u^* = \frac{z}{\|z\|},$$

where  $z \sim \mathcal{N}(0, I_d)$ . We want to lower bound  $\sum_{i=1}^m \sigma_i^2 [U^\top w^*]_i^2 = \sum_{i=1}^m \sigma_i^2 (u_i^*)^2$ . We can write

$$\sum_{i=1}^m (u_i^*)^2 \sigma_i^2 = \frac{\sum_{i=1}^m z_i^2 \sigma_i^2}{\sum_{i=1}^m z_i^2}.$$

Thus we need to get the upper bound of  $\sum_{i=1}^m z_i^2$  and the lower bound of  $\sum_{i=1}^m z_i^2 \sigma_i^2$ . Note that

$$1 = \sigma_1 \geq \sigma_2 \geq \dots \sigma_r > 0.$$

Since  $z_i \sim \mathcal{N}(0, 1)$ ,  $X = \sum_{i=1}^m z_i^2$  is 1-sub-exponential r.v. with expectation 1. Thus, with Bernstein inequality (i.e., see Theorem 2.8.1 in (Vershynin, 2018)), for  $\epsilon > 0$ , we have that:

$$\begin{aligned} \mathbb{P} \left( \sum_{i=1}^m \sigma_i^2 z_i^2 \leq \sum_{i=1}^m \sigma_i^2 - \epsilon m \right) &\leq \mathbb{P} \left( \left| \frac{1}{m} \sum_{i=1}^m \sigma_i^2 z_i^2 - \frac{1}{m} \sum_{i=1}^m \sigma_i^2 \right| \leq \epsilon \right) \\ &\leq 2 \exp \left( -c \min \left( \frac{\epsilon^2 m^2}{\sum_{i=1}^m \sigma_i^4}, \frac{\epsilon m}{\max_i \sigma_i^2} \right) \right) \\ &\leq 2 \exp \left( -c \min \left( \frac{\epsilon^2 m^2}{\sum_{i=1}^m \sigma_i^2}, \frac{\epsilon m}{\max_i \sigma_i^2} \right) \right) \quad \text{since } \sum_{i=1}^m \sigma_i^2 \geq \sum_{i=1}^m \sigma_i^4 \end{aligned} \quad (46)$$

and

$$\mathbb{P} \left( \sum_{i=1}^m z_i^2 \geq (1 + \epsilon)m \right) \leq \mathbb{P} \left( \left| \frac{1}{m} \sum_{i=1}^m (z_i^2 - 1) \right| \geq \epsilon \right) \leq 2 \exp(-c \min\{m\epsilon^2, m\epsilon\}). \quad (47)$$

where  $c$  is an absolute constant.

Let  $\epsilon = \sqrt{\frac{\log(m)}{m}} \leq 1$ . Then,  $\epsilon^2 m \leq \frac{\epsilon^2 m^2}{\sum_{i=1}^m \sigma_i^2} < \frac{\epsilon m}{\max_i \sigma_i^2} = \epsilon m$  since  $2\sqrt{m \log m} < \sum_i \sigma_i^2$ . Thus equation 46 and equation 47 can be simplified, respectively,

$$\mathbb{P}\left(\sum_{i=1}^m \sigma_i^2 z_i^2 \leq \sum_{i=1}^m \sigma_i^2 - \sqrt{m \log(m)}\right) \leq \exp(-cm\epsilon^2) = \frac{1}{m} e^{-c} = \mathcal{O}\left(\frac{1}{m}\right) \quad (48)$$

and

$$\mathbb{P}\left(\sum_{i=1}^m z_i^2 \geq m + \sqrt{m \log(m)}\right) \leq \frac{1}{m} e^{-c} = \mathcal{O}\left(\frac{1}{m}\right). \quad (49)$$

Then with probability  $1 - \mathcal{O}\left(\frac{1}{m}\right)$ , we have

$$\sum_{i=1}^m (u_i^*)^2 \sigma_i^2 = \frac{\sum_i z_i^2 \sigma_i^2}{\sum_{r=1}^m z_r^2} \geq \frac{\sum_{i=1}^m \sigma_i^2 - \sqrt{m \log(m)}}{m + \sqrt{m \log m}} \geq \frac{1}{m} \sum_{i=1}^m \sigma_i^2 - 2\sqrt{\frac{\log(m)}{m}} \geq \sigma_m^2$$

where the last inequality is due to the assumption that the spectral satisfies  $\frac{1}{m} \sum_{i=1}^m \sigma_i^2 > 2\sqrt{\frac{\log(m)}{m}} + \sigma_m^2$ . To sum up, with probability  $1 - \mathcal{O}\left(\frac{1}{m}\right)$ ,

$$\sum_{i=1}^m \sigma_i^2 [u^*]_i^2 \geq \frac{1}{m} \sum_{i=1}^m \sigma_i^2 - 2\sqrt{\frac{\log(m)}{m}} = \frac{1}{m} \left( \|AA^\top\|_F^2 - 2\sqrt{m \log(m)} \right)$$

Now, using the derivation in equation 45 for lower bound of  $\|v_t\|$ , we have that:

$$\begin{aligned} \|v_t\| &\geq \frac{g^*}{g_0} \sqrt{\frac{\|AA^\top\|_F^2 - 2\sqrt{m \log(m)}}{m}} - (1 - \sigma_m) \geq 1 + \delta \\ \Rightarrow g_0 &\leq \frac{g^*}{(2 + \delta - \sigma_m)} \sqrt{\frac{\|AA^\top\|_F^2 - 2\sqrt{m \log(m)}}{m}} \end{aligned}$$

With  $g_0$  satisfying above, we can guarantee that  $\|v_t\| \geq 1 + \delta$ .

□